ISSN 0869-5938, Stratigraphy and Geological Correlation, 2015, Vol. 23, No. 2, pp. 155–191. © Pleiades Publishing, Ltd., 2015.
Original Russian Text © V.V. Arkadiev, E.Yu. Baraboshkin, M.I. Bagaeva, T.N. Bogdanova, A.Yu. Guzhikov, A.G. Manikin, V.K. Piskunov, E.S. Platonov, Yu.N. Savel'eva, A.A. Feodorova, O.V. Shurekova, 2015, published in Stratigrafiya. Geologicheskaya Korrelyatsiya, 2015, Vol. 23, No. 2, pp. 43–80.

# New Data on Berriasian Biostratigraphy, Magnetostratigraphy, and Sedimentology in the Belogorsk Area (Central Crimea)

**V. V. Arkadiev[a], E. Yu. Baraboshkin[b], M. I. Bagaeva[c], T. N. Bogdanova[d], A. Yu. Guzhikov[c], A. G. Manikin[c], V. K. Piskunov[b], E. S. Platonov[a], Yu. N. Savel'eva[e], A. A. Feodorova[e], and O. V. Shurekova[e]**

[a] *St. Petersburg State University, Universitetskaya nab. 7–9, St. Petersburg, 199034 Russia*
*e-mail: arkadievvv@mail.ru*
[b] *Moscow State University, Moscow, 119991 Russia*
[c] *Saratov State University, ul. Astrakhanskaya 83, Saratov, 410012 Russia*
[d] *All-Russian Institute of Geology, Srednii pr. 74, St. Petersburg, 199106 Russia*
[e] *Research and Production Enterprise Geologorazvedka, ul. Knipovicha 11/2, St. Petersburg, 192019 Russia*

Received July 9, 2013; in final form, December 17, 2013

**Abstract**—The most complete composite Berriasian bio- and magnetostratigraphic section of central Crimea is characterized for the first time with a description of the contact between the carbonate Bedenekyr and terrigenous Bechku formations. The section contains all the standard ammonite zones: jacobi, occitanica, and boissieri. The Malbosiceras chaperi Beds are attributed to the occitanica Zone. The Berriasian section is characterized by six foraminiferal assemblages, ostracods (Costacythere khiamii–Hechticythere belbekensis and Costaythere drushchitzi–Reticythere marfenini beds), and dinocysts (Phobercysta neocomica Beds). The magnetostratigraphic section contains analogs of Chrons M17 and M16 reliably correlated with ammonite zones. On the basis of paleomagnetic data, the Berriasian section of central Crimea is correlated with coeval sections of the Mediterranean Region. The sedimenological analysis confirms accumulation of Berriasian sediments mostly in shallow shelf environments of the carbonate platform.

*Keywords*: Berriasian, central Crimea, ammonites, bivalves, ostracods, foraminifers, palynomophs, biostratigraphy, magnetostratigraphy, sedimentology, paleomagnetism, magnetic polarity, magnetic chrons

**DOI:** 10.1134/S0869593815020033

## INTRODUCTION

The Berriasian sections in the central part of the Crimean Peninsula were investigated by many researchers (Drushchits and Yanin, 1959; Kvantaliani and Lysenko, 1979; Bogdanova et al., 1981; Bogdanova and Kvantaliani, 1983; etc.); their paleomagnetic study was first conducted by V.N. Eremin in the 1980s (Molostovskii et al., 1989). The evolution of views on their subdivision is considered in detail in the recently published collective monograph (Arkadiev et al., 2012). We conducted complex bio- and magnetostratigraphic investigations of Berriasian sections in central Crimea in 2002 and 2011–2012. In 2002, a team of geologists from Moscow and Saratov State Universities examined sections near the settlements of Balki and Pasechnoe. Unfortunately, fragmentary magnetostratigraphic records were obtained only for the Pasechnoe section. No paleomagnetic measurements appropriate for interpretation of magnetic polarity were obtained for the Balki section because of insufficient sensitivity of the laboratory equipment used at that time (Yampolskaya, 2005).

The joint efforts of specialists from St. Petersburg, Saratov, and Moscow State Universities and Research and Production Enterprise *Geologorazvedka* resulted in the complex investigation of sections in the outskirts of the settlements of Balki, Mezhgor'e, and Novoklenovo in 2011 and sections in the Enisarai Ravine and on the northern slope of the Karabi-Yaila Plateau (south-southwest of the Balki settlement) in 2012 (Fig. 1). The field works were dedicated to the thorough description of sections (including the contact between limestones of the Bedenekyr Formation and sandy–clayey Bechku Formation first discovered at two localities in the outskirts of the Balki settlement), sampling of organic remains (ammonites, bivalves, corals) and rocks for the study of micro- (foraminifers, ostracods, dinocysts, calpionellids, spores, and pollen) and ichnofossils, paleomagnetic measurements, and sedimentological analysis. The subsequent analysis of sampled material made it possible, first, to correlate isolated outcrops between each other and compile the most complete Berriasian section for central Crimea and, second, to obtain its micropaleontological and magentostratigraphic characteristics. The lithological description of

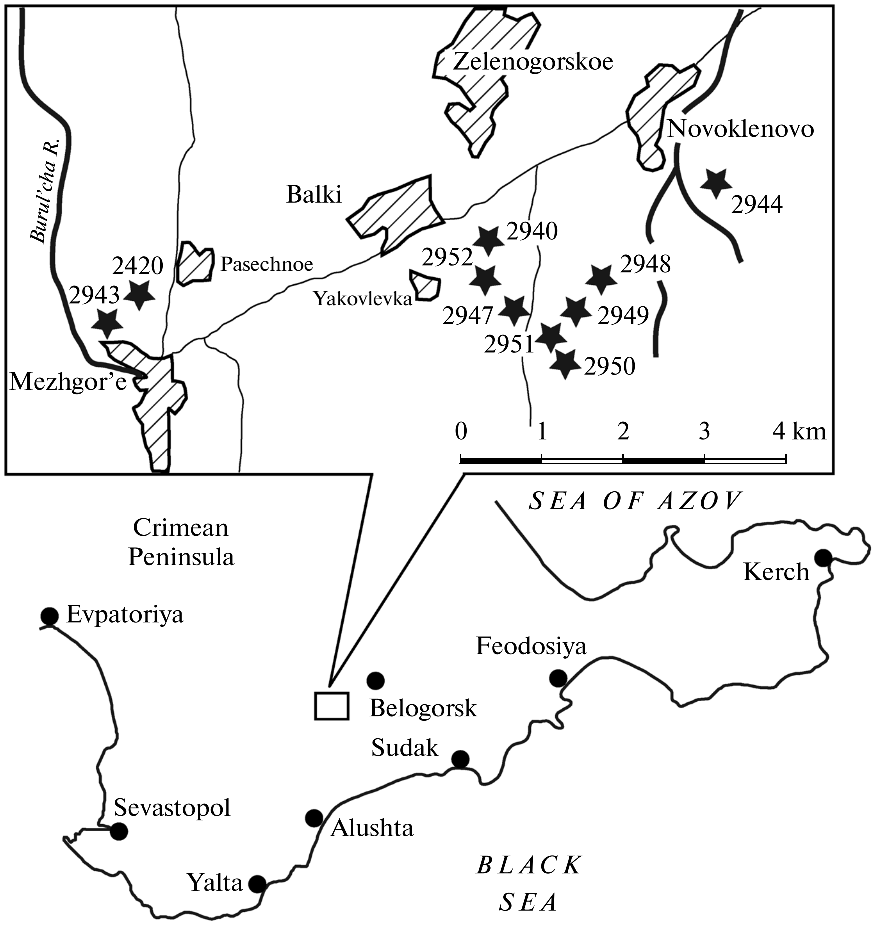


**Fig. 1.** Location of Berriasian outcrops in the Sary-Su River basin. Numerals correspond to section numbers.

the section was accomplished by E.Yu. Baraboshkin and V.K. Piskunov. The paleomagnetic data were obtained by M.I. Bagaeva, A.Yu. Guzhikov, and A.G. Manikin. Organic remains were identified by the following specialists: ammonites by V.V. Arkadiev and T.N. Bogdanova; bivalves by T.N. Bogdanova; brachiopods and echinoderms by S.V. Lobacheva; corals by I.Yu. Bugrova; crinoids by V.G. Klikushin; ostracods by Yu.N. Savel'eva; dinocysts, spores, and pollen by O.V. Shurekova; foraminifers by A.A. Feodorova; ichnofossils by E.Yu. Baraboshkin. E.S. Platonov made an attempt to find calpionellids in thin sections (200 in total), but failed. The ammonite specimen, foraminifers, and ostracods illustrated in this work (collection no. 13244) are stored at the Central Research Geological Museum (St. Petersburg); the collection of palynomorphs (no. 13220) is stored at the same place.

## STRUCTURE OF THE SUCCESSION

In the Sary-Su River basin (Mezhgor'e–Balki–Novoklenovo settlement area) (Fig. 1), the Berriasian Stage includes (from the base upward) limestones and clayey limestones of the upper Bedenekyr Formation, siltstones and sandstones of the Bechku Formation, and sponge horizon, clays, siltstones, and biohermal limestones of the Kuchki Formation (Arkadiev, 2007). According to (Bogdanova et al., 1981), limestones of the Bedenekyr Formation cropping out south of the Balki Settlement on the Karabi-Yaila Plateau contain ammonites *Pseudosubplanites ponticus* (Ret.) and *Berriasella jacobi* (Maz.) of the jacobi zone. Unfortunately, more exact localization of these ammonite forms remains unknown. It is conceivable that E.Yu. Baraboshkin investigated the same section or its analogs on the northwestern slope of the Karabi-Yaila Plateau in the vicinity of the military camp in 1996–1997. In this area, white and pinkish upper Tithonian bioclastic limestones with *Anchispirocyclina lusitanica* (Egger) are overlain by white limestones at least 50–60 m thick with ammonites *Berriasella* sp. and *Protetragonites tauricus* (Kulj.-Vor.), brachiopods *Loriolithyris* sp., bivalves *Gervilella* sp. and *Pinna* sp., and gastropods.

The Bechku Formation in central Crimea is characterized by ammonites *Dalmasiceras tauricum* (Bogd. et Ark.), *Malbosiceras chaperi* (Pict.), *M. malbosi* (Pict.), *M. pictetiforme* Tav., *Neocosmoceras euthymi* (Pict.), *N. minutus* Ark. et Bogd., *Hegaratia bidi-*

*chotoma* Bogd. et. Kvant., *Fauriella simplicicostata* (Maz,), *F. boissieri* (Pict.), and others.[1] On the basis of this ammonite assemblage, the Bechku Formation was correlated with the jacobi (Malbosiceras chaperi Beds), occitanica, and boissieri zones. No guide ammonite species were found in the Kuchki Formation developed in the Sary-Su River basin. The sponge horizon contains abundant brachiopod remains belonging to *Symhythiris arguinensis* (Moiss.), which is characteristic of the synonymous beds. Ammonites in the horizon are represented only by *Hegaratia* sp. and *Spiticeras* sp. In 2002, E.Yu. Baraboshkin found in its basal layer *Riasanites crassicostatum* (Kyant. et Lys.) together with *Loriolithyris valdensis* (Lor.) and *Symphythiris arguinensis* (Miss.). This find allows at least the base of the sponge horizon to be attributed to the crassicostatum Subzone. The siltstone member overlying the sponge horizon near the settlement of Mezhgor'e yielded rare poorly preserved ammonites: *Haploceras* ex gr. *cristifer* (Opp.), *Protetragonites tauricus* (Kulj.-Vor.), *Spiticeras* sp., and *Subalpinites* sp. (identifications by T.N. Bogdanova). These species of the genera *Haploceras, Protetragonites*, and *Spiticeras* occur through the entire Berriasian section of Crimea. In France, representatives of the genus *Subalpinites* are known from all the Berriasian zones (Le Hégarat, 1973). In Crimea, the *Sualpinites* taxa are described by V.V. Arkadiev (Arkadiev et al., 2012) from the occitanica Zone in the outskirts of the Balki settlement. Nevertheless, the stratigraphic position of beds and their ammonites are consistent also with their attribution to the boissieri Zone. The biohermal limestones occurring in the upper part of the section are barren of ammonite remains. Therefore, in the previously proposed stratigraphic scale (Arkadiev et al., 2012), they are conditionally attributed to the Berriasian. At the same time, finds of brachiopods *Symphythiris kojnautensis* (Moiss.), *Weberithyris moissevi* (Weber), *Zeillerina baksanensis* Smirn., bivalves *Megadiceras koinautense* Pchel., and others in this sequence have been known for a long time (Yanin and Smirnova, 1981). The correlation of these limestones with the Bel'bek River section, where similar facies and faunal assemblages occur below the undoubtedly lower Valanginan layers, allows this sequence to be attributed to the upper Berriasian Megadiceras koinautense Beds (Yanin and Baraboshkin, 2000).

The upper surface of limestones is eroded and affected by karst processes; the rocks are crossed by deep (over 6 m) cracks filled with quartz sandstone. The change in the sedimentation patterns in southwestern Crimea is typical of the Berriasian–Valanginian transition.

The total thickness of the Berriasian section in the Sary-Su River basin is approximately 600 m (taking into consideration gaps in observations). Unfortunately, the section does not represent a continuous succession and is investigated in isolated outcrops correlated on the basis of faunal finds. In the examined sections, the layers dip at an angle of 10°–12° in the NNE direction.

Below, we describe the lithological composition of fragments constituting the composite section, some of which are well known (outcrops 2420, 2940, 2943, 2944, 2947), while others were visited for the first time (outcrops 2948–2952). All these outcrops are located in the outskirts of the Balki, Mezhgor'e, and Novoklenovo settlements (Fig. 2).

*Section 2950 (44°58′36.40″ N, 34°28′45.90″ E; Fig. 3)*

Member 1 (Samples 2950/1–5). Yellowish gray bedded bioclastic wacke- to, less commonly, packstones with abundant thalassinoid burrows. Limestones contain ooids, bioclasts of brachiopod and bivalve shells, skeletal detritus, and single foraminiferal tests of the *Everticyclammina virguliana–Retrocyclammina recta–Bramkampella arabica* Assemblage. The thickness is 4.5 m.

*Section 2951 (44°58′41.40″ N, 34′28°44.50″ E; Fig. 3)*

Member 2 (Samples 2951/1–7). Wacke- and packstones similar to rocks constituting Member 1. The talus yielded ammonite *Malbosiceras* ex gr. *malbosi* (Pictet). The thin sections demonstrate abundant sections of foraminifers belonging to the *Everticyclammina virguliana–Retrocyclammina recta–Bramkampella arabica* Assemblage. The thickness is 12 m.

*Section 2947 (Enisarai; 44°58′54.80″ N, 34°28′18.00″ E; Fig. 3)*

The lower part of the section is similar to Member 2 (Samples 2947/1–9). These sediments are overlain by the following units:

Member 3 (Samples 2951/9–40). Gray bedded packstones and, less commonly, wackestones (layers 10–50 cm thick) with abundant *Thalassinoides* burrows, skeletal detritus up to 2 mm across, and rare larger bioclasts. The boundaries between layers are wavy. The layers contain abundant ferrugenous ooids and substantially rarer marcasite concretions. The taluses from the lower and upper parts of the member yielded bivalves *Prohinnites renevieri* (Coq.) and *Tortarctica weberae* Mordv., respectively. The thin sections exhibit abundant sections of foraminifers of the *Everticyclammina virguliana–Retrocyclammina recta–Bramkampella arabica* Assemblage. The thickness is 63 m.

*Section 2949 (44°58′56.10″ N, 34°28′59.10″ E; Fig. 3)*

This section comprises five members (from the base to the top):

Member 4 (Samples 2949/1–3). Thick-bedded (30–40 cm) packstones with ferruginous ooids, bio-

[1] E.Yu. Baraboshkin believes that species *euthymi* and *minutus* should be attributed to the genus *Euthymiceras*, and species *bidichotoma* and *nerodenkoi*, to the genus *Balkites*.

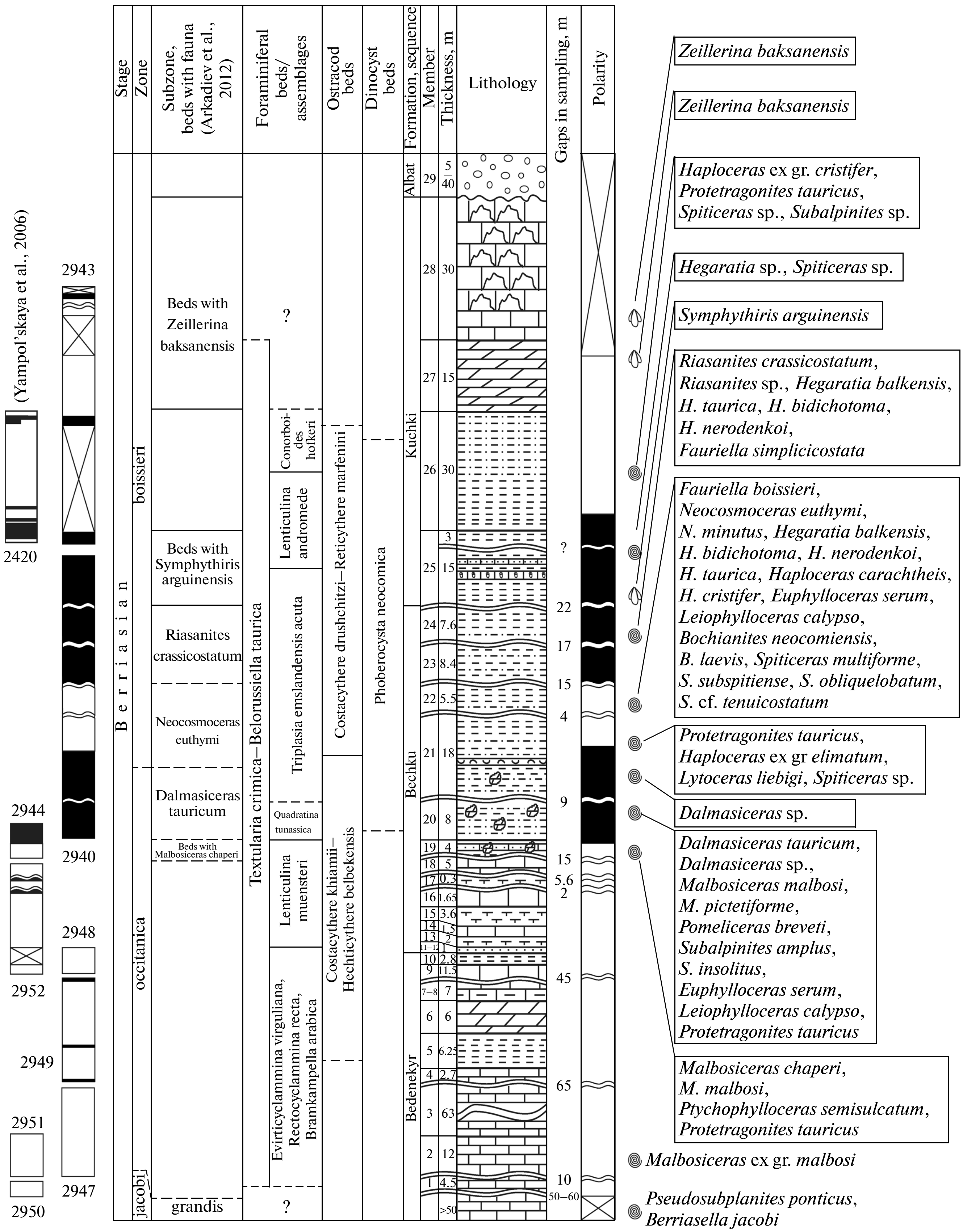


**Fig. 2.** Composite bio- and magnetostratigraphic Berriasian section of central Crimea. For legend, see Fig. 4.

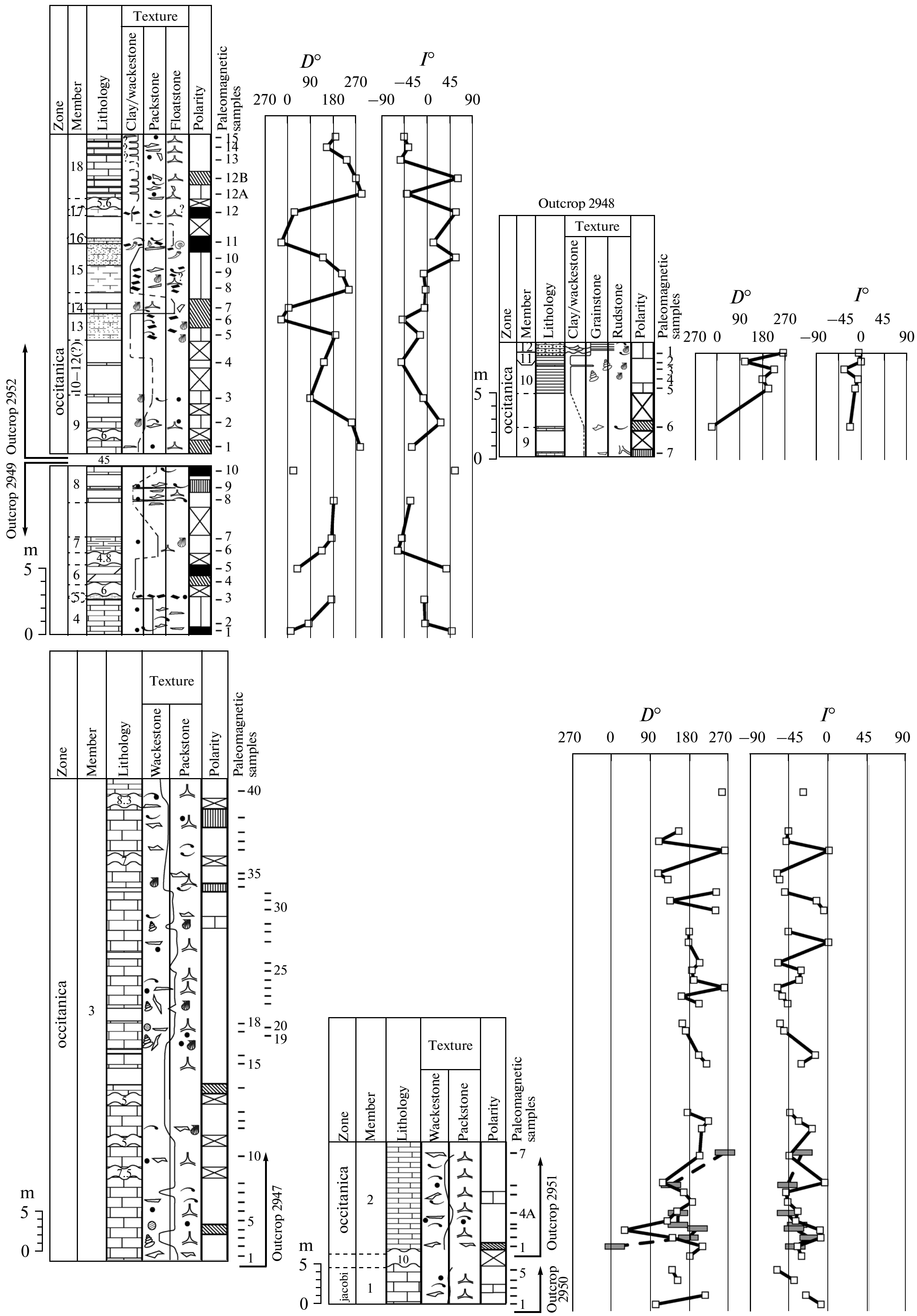


**Fig. 3.** Lithological–sedimentological and paleomagnetic data on outcrops 2947–2952. For legend, see Fig. 4.

clast detritus up to 2 mm across, and rare larger bioclasts. The rocks contain intact shells of bivalves *Tortarctica weberae* Mordv. The thin section contains rare sections of foraminifers belonging to the *Everticyclammina virguliana–Retrocyclammina recta–Bramkampella arabica* Assemblage The thickness is 2.7 m.

Member 5. Gray clays containing carbon detritus, ferruginous ooids, abundant foraminifers of the *Everticyclammina virguliana–Retrocyclammina recta–Bramkampella arabica* Assemblage, and ostracods *Cytherella lubimovae* Neale, *Cytherelloidea mandelstami* Neale, *Costacythere khiamii* Tes. et Rach.), *C. foveata* Tes. et Rach, *Hechticythere belbekensis* Tes. et Rach., *Quasigermanites bicarinatus moravicus* Pok., and others. They are accompanied by single spores and pollen grains, dinocysts of the *Muderongia* Assemblage, and prasinophytes. The thickness is 0.25 m.

Further, there is an unexposed interval 6 m wide.

Member 6 (Samples 2949/4–5). Light gray bedded marlstones (layers of approximately 20 cm thick) with foraminifers of the *Everticyclammina virguliana–Retrocyclammina recta–Bramkampella arabica* Assemblage with calcareous forms characterized by dwarfish sizes. The ostracod assemblage consists of *Cytherella krimensis* Neale, *C. lubimovae* Neale, *C. fragilis* Neale, and others. The microfossils include also single spores, pollen, and dinocysts of the *Muderonia* assemblage. The thickness is 1.2 m.

There is an unexposed interval 4.8 m wide.

Member 7 (Samples 2949/6–7). Light gray clayey limestones with *Thalassoinoides* burrows and single ferruginous ooids. The thin sections exhibit single sections of foraminifers from the *Everticyclammina virguliana–Retrocyclammina recta–Bramkampella arabica* Assemblage. The thickness is 1 m.

There is an unexposed interval 3 m wide.

Member 8 (Samples 2949/8–10) is poorly exposed, being represented by isolated outcrops of gray wacke- and packstones 0.3–0.4 m thick with ferruginate ichnofossils (*Thalassinoides*?), skeletal detritus, unidentifiable bivalve shells, and ferruginous oolites. The two upper layers enclose lenses of shelly floatstones. The thin section demonstrates single foraminifers belonging to the *Everticyclammina virguliana–Retrocyclammina recta–Bramkampella arabica* Assemblage. The thickness is 3 m.

### *Section 2948 (44°59′00.06″ N, 34°29′10.50″ E; Fig. 3)*

The section comprises seven members (from bottom to top):

Member 9 (Samples 2948/6–7) is poorly exposed, being represented by two outcrops of gray wacke- and packstones (0.2–0.3 m thick) with rare *Thalassinoides* burrows. Thin sections yield foraminifers of the impoverished *Everticyclammina virguliana–Retrocyclammina recta–Bramkampella arabica* Assemblage and ostracods represented by *Costacythere andreevi* Tes., *C. khaimii* Tes. et Rach., *Quasigermanites bicarinatus moravicus* Pok., and others. They are accompanied by dinocysts from the *Mudergonia* Complex, *Systematophora areolata* Klement, *Kleithriasphaeridium eoinodes* (Eisenback), *Prolixosphaeridium parvispinum* (Deflandre), *Achomosphaera* sp., and *Cometodinium habibii* Montail. The thickness is 11.5 m.

There is an unexposed interval 2.7 m wide.

Member 10 (Samples 2948/2–5) is composed of gray clays (layers 20–50 cm thick) with intercalations of dark clays (up to 2–3 cm). Some levels yielded ferruginate unidentifiable casts of gastropod and bivalve shells. The middle part of the member encloses a single lens-shaped intercalation of light gray grainstones with gastropod shells, impoverished *Everticyclammina virguliana–Retrocyclammina recta–Bramkampella arabica* foraminiferal assemblage dominated by simple lituolids and poorly preserved *Lenticulina* tests, and ostracods *Costacythere khaimii* Tes. et Rach. and others. The thickness is 2.8 m.

Member 11. Yellowish gray slightly consolidated sandstone with foraminifers of the *Everticyclammina virguliana–Retrocyclammina recta–Bramkampella arabica* Assemblage and ostracods *Costacythere khiamii* Tes. et Rach., *Hechticythere belbekensis* Tes. et Rach., *Schuleridea* ex gr. *juddi* Neale, and others. The thickness is 0.2 m.

Member 12 (Sample 2948/1) is composed of horizontally bedded mixed carbonate–terrigenous sandstones with an incised channel filled with trough cross-bedded sediments containing bivalve shells, which are oriented parallel to bedding surfaces and saturate some laminae. The sandstones contain rare crustacean *Ophiomorpha* sp. burrows. Bivalves are represented by *Prohinnites renevieri* (Coq.) and *Entolium germanicum* (Woll.). The member yielded also a fragment of ammonite *Fauriella* (?) sp. and foraminifers of the impoverished *Everticyclammina virguliana–Retrocyclammina recta–Bramkampella arabica* Assemblage age dominated by simple lituolids and poorly preserved *Lenticulina* tests, ostracods *Costacythere khiamii* Tes. et Rach., *Hechticythere belbekensis* Tes. et Rach., *Schuleridea* ex gr. *juddi* Neale, and others, and dinocysts *Spiniferites* ex gr. *ramosus* (Ehren.). The thickness is 0.8 m.

### *Section 2952 (44°59′09.24″ N, 34°28′13.36″ E; Fig. 3)*

Similar to Section 2948, this section 2952 encloses the contact between the calcareous and terrigenous sequences. On the basis of this feature, its lower part is correlated with the former section.

Member 9 (Samples 2952/1–3) is poorly exposed, being represented by isolated outcrops of gray wacke- and packstones 0.2–1.0 m thick with thalassinoid burrows, ferruginous ooids, bioclast detritus up to 2 mm across, less common larger biocalsts, and intact bivalve shells. The sediments are frequently ferruginate along bedding surfaces. The thickness is 11.5 m.

There is an unexposed interval 4 m wide with a single intercalation of packstone, which represents presumably an analog of grainstone in Member 10 (Sample 2952/4) of Section 2948. The thin sections exhibit single sections of foraminifers *Melathrokerion spirialis* Gorb.

M e m b e r 13 (Samples 2952/5–6) is composed of light greenish gray calcareous clays with sand admixture, carbon detritus, intact unidentifiable casts of bivalve shells, and their fragments. The rocks contain the foraminifers of the *Lenticulina muensteri* Assemblage. Many *Lenticulina* shells are poorly preserved. Simple lituolids demonstrate gigantism. The ostracod assemblage includes *Costacythere khiamii* Tes. et Rach., *C. foveata* Tes. et Rach., *Hechticythere belbekensis* Tes. et Rach., and others. Microphytoplankton is represented by unidentifiable proximate dinocysts and prasinophytes. The thickness is 2 m.

M e m b e r 14 (Sample 2952/7) is represented by light gray bioturbated floatstones with intact unidentifiable bivalve casts covered by vague encrustations and shell detritus. The thickness is 0.7 m.

There is an unexposed interval 0.75 m wide.

M e m b e r 15 (Samples 2952/8–10) consists of greenish gray calcareous clays with abundant carbon detritus, shelly detritus, and ferruginate structures (bioturbation?). Accumulations of bivalve shells form coquina. Bivalves are represented by *Gervillella anceps* (Desh. et Leym.), *Neithea simpliex* Mordv., and *Integricardium deshayesianum* (Lor.). Up the section, clays become sandy and contain abundant solitary corals *Montlivaltia crimea* Kusm. The upper 0.5 m of the member is poorly exposed and contains carbon detritus, and single unidentifiable remains of ammonites, belemnites, bivalves *Gervillella anceps* (Desh. et Leym.) and *Neithea simpliex* Mordv., and foraminifers of the *Lenticulina muensteri* Assemblage with single planktonic forms. The representatives of this assemblage are dwarfish and abnormal in shape. Many *Lenticulina* and *Hoeglundina* tests are poorly preserved. The ostracod assemblage includes *Costacythere khiamii* Tes. et Rach., *C. foveata* Tes. et Rach., *C. drushchitzi* (Neale), and other species. There are also spores of Schizaleales ferns *Lygodium* sp. and bisaccate coniferous and *Classopollis* spp. pollen. The thickness is 3.6 m.

M e m b e r 16 (Sample 2952/11) is poorly exposed, being represented by sandy floatstones with unidentifiable bivalve shells. The thickness is 0.4 m.

There is an unexposed interval 1.65 m wide.

M e m b e r 17 (Sample 2952/12) is composed of slightly calcareous clays with carbon detritus, shelly detritus, and ferruginate structures (sediment feeding burrows?). The foraminiferal *Lenticulina muensteri* Assemblage includes dwarfish forms. Ostracods are represented by *Cytherella krimensis* Neale, *C. flexuosa* Neale, *Pontocypris felix* Neale, and other species. The sediments contain also bisaccate coniferous pollen. The thickness is 0.3 m.

There is an unexposed interval approximately 5.6 m wide.

M e m b e r 18 (Samples 2952/12A–15) consists of weathered pack- and wackestones with vague (due to poor exposure) clay intercalations (5–15 cm thick). The pack- and wackestones demonstrate thalassinoid burrows, skeletal detritus, and single ferruginous ooids. They contain foraminifers of the *Everticyclammina virguliana–Retrocyclammina recta–Bramkampella arabica* Assemblage dominated by *Melathrokerion spirialis* Gorb. The ostracod assemblage includes *Cytherella lubimovae* Neale, *Cytherelloidea mandelstami* Neale, *Costacythere khiamii* Tes. et. Rach., *C. foveata* Tes. et Rach., *Hechticythere belbekensis* Tes. et Rach., *Reticythere marfenini* Tes. et Rach., *Schuleridea* ex gr. *juddi* Neale, and other forms. The middle part of the member is unexposed (interval 1.2 m wide). The thickness is 5 m.

The X-ray phase analysis of clay samples from Sections 2948, 2949, and 2952 revealed that all of them are characterized by a practically identical composition: quartz, calcite, and minerals of the kaolinite group, mica, chlorite, rarely albite, anorthite, and gibbsite. A single sample yielded dolomite. The samples were analyzed with a Rigaku MiniFlex II diffractometer.

### *Section 2944 (Novoklenovo; 44°59′46.80″ N, 34°30′16.40″ E; Fig. 4)*

M e m b e r 19 (Samples 2944/1–3) is largely composed of yellow to brown unconsolidated clayey siltstones and brownish gray clays. The lower part of analogs of this member near the Balki settlement contains an intercalation of brown calcareous sandstones (0.4 m thick) with compact marlstone concretions, which yielded ammonites *Malbosiceras chaperi* (Pict.), *M. malbosi* (Pict.), and others; bivalves *Entolium germanicum* (Woll.), *Aetostreon subsinuatum* Leym., and *Integricardium deshayesianum* (Lor.); and brachiopods *Sellithyris* cf. *uniplicata* Smirn. The thickness is 4 m.

M e m b e r 20 (Samples 2944/4–9, Novoklenovo; Samples 2940/1–7, Balki) consists of brown clays and siltstones with marlstone concretions. Near the Novoklenovo settlement, the member yielded ammonites *Dalmasiceras tauricum* Bogd. et Ark. and its analogs near the Balki settlement, *Dalmasiceras tauricum* Bogd. et Ark., *Malbosiceras malbosi* (Pict.), *M. pictetiforme* Tav., *Pomeliceras breveti* (Pom.), *Subalpinites amplus* Ark., *S. insolitus* Ark. and others; bivalves *Pycnodonte weberae* Yanin; and brachiopods *Loriolithyris* cf. *valdensis* (Lor.) and *Sellithyris* ex gr. *gratianopolitensis* (Pict.). The member contains also diverse microfossils: foraminifers of the *Quadratina tunassica* Assemblage; ostracods *Cytherelloidea flexuosa* Neale, *Pontocyprella nova* Neale, *Cypridea funduklensis* Tes. et. Rach., *Acrocythere alexandrae* Neale et Kolp., and other forms; single spores and *Classopollis* spp. pollen; dinocyst of the *Phoberocysta neocomica* Assemblage; prasinophytes; and acritarchs. The thickness is 8 m.

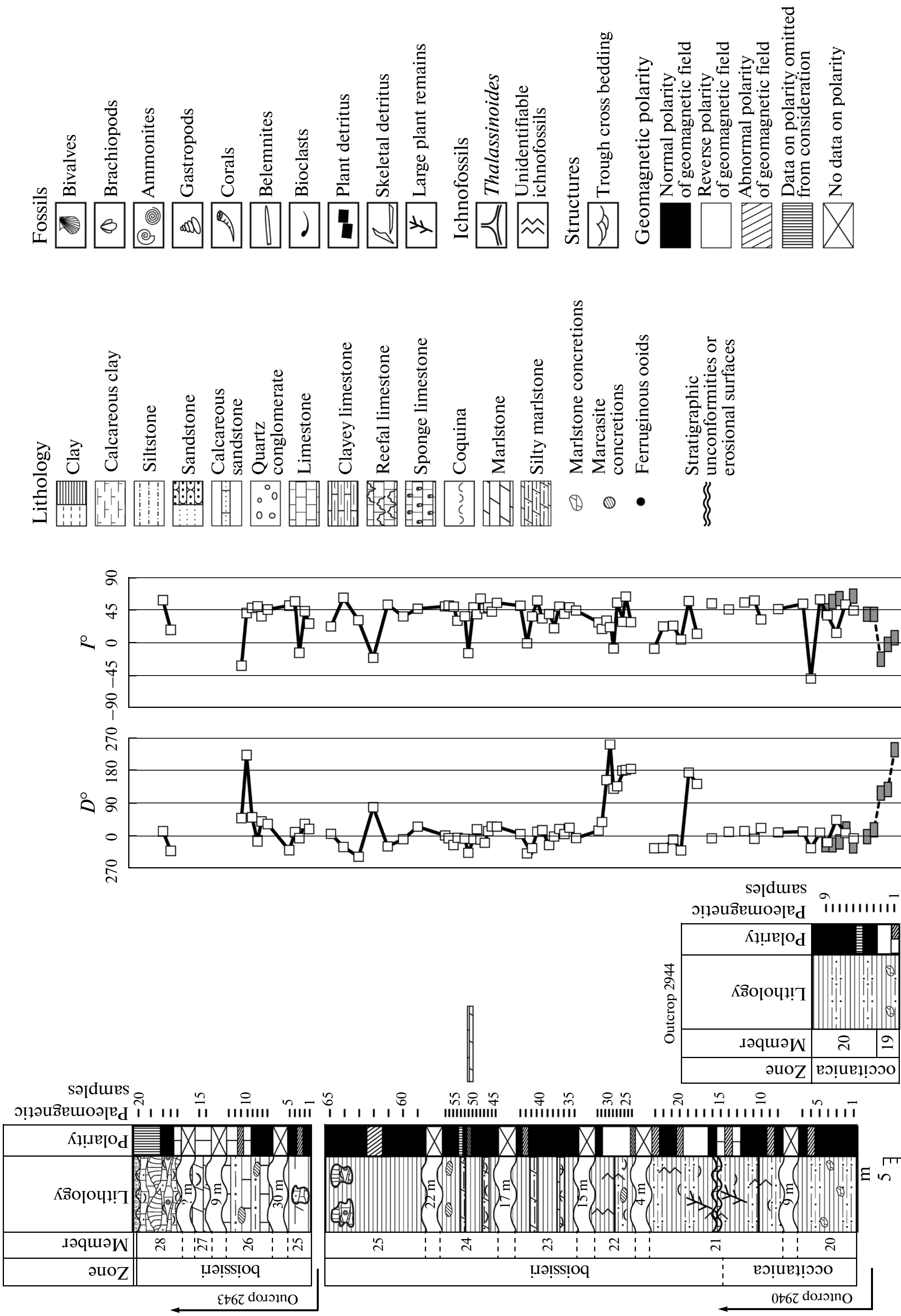


**Fig. 4.** Lithological–sedimentological and paleomagnetic data on outcrops 2940, 2943, and 2944.

*Section 2940 (Balki; 44°59′21.94″ N, 34°28′07.11″ E; Fig. 4)*

Member 21 (Samples 2940/8–23) comprises dark gray, dark brown, and brown-gray (dominant) clays with rare marlstone concretions and greenish gray calcareous siltstones. In its middle part, the member encloses several intercalations (0.15–0.20 cm thick) of calcareous siltstones representing oyster accumulations with *Pycnodonte weberae* Yanin. The member contains diverse macro- and microfossils: ammonites *Dalmasiceras* sp. in its lower part; ammonites *Protetragonites tauricus* (Kulj.-Vor.), *Haploceras* ex gr. *elimatum* (Opp.), *Lytoceras liebigi* (Opp.), and *Spiticeras* sp. in the upper part; bivalves *Entolium germanicum* (Woll.), *Spondylus complanatus* (d'Orb.), and others; brachiopods *Loriolithyris valdenses* (Lor.), *Sellithyris uniplicata* Smirn., *Belbekella airgulensis* Moiss, and other species; foraminifers of the *Triplasia emslandensis acuta* Assemblage (some layers contain giant agglutinated forms and planktonic species); ostracods *Pontocypris cuneata* Neale, *Acrocythere alexandrae* Neale et Kolp., *Costacythere khiamii* Tes. et Rach., *Hechticythere belbekensis* Tes. et Rach., and *Reticythere marfenini* Tes. et Rach.; single spores including Schizaleales ferns *Cicatricosisporites* sp. and pollen of *Classopolllis* spp.; dinocysts of the *Phoberocysta neocomica* Assemblage. The thickness is 18 m.

Member 22 (Samples 2940/24–33) is composed of dark greenish gray and brown (dominant) viscous clays and dark gray and brownish siltstones. The member contains different organic remains scattered through its entire sections: abundant small ferruginate casts of ammonites *Neocosmoceras euthymi* (Pict.), *N. minutus* Ark. et Bogd., *Hegaratia bidichotoma* (Bogd. et Kvant.), *H. nerodenkoi* (Bogd. et Kvant.), *H. balkensis* (Bogd. et Kvant.), *Spiticeras multiforme* Djan., *S. subspitiense* (Uhl.), *S. obliquelobatum* (Uhl.), *Bochinites neocomiensis* (d'Orb.), *B. laevis* Liu, and others (*Fauriella boissieri* (Pictet) from the collection by V.V. Drushchits originates likely from the same member); bivalves *Pycnodonte weberae* Yanin, *Aetostreon subsinuatum* (Leym.), and others; brachiopods *Loriolithyris valdensis* (Lor.), *Symphythiris arguinensis* (Moiss.), *Terebratuliopsis quadrata quadrata* Smirn., and other forms; rare foraminifers from the impoverished *Triplasia emslandensis acuta* assemblage; ostracods *Cytherelloidea flexuosa* Neale, *Bythoceratina* ex gr. *variabilis* Donze, *Eucytherura* aff. *trinodosa* Pok., and others; spores of Schizaleales ferns *Cicatricosisporites* sp., pollen of *Classopolllis* spp., and prasinophytes. The thickness is 5.5 m.

Member 23 (Samples 2940/34–44) is represented by dark greenish gray and brown clays alternating with dark gray siltstones. The member contains the impoverished *Triplasia emslandensis acuta* Assemblage with dominant *Spirillina kubleri* Mjatl. and ostracods *Cytherella krimensis* Neale, *C. fragilis* Neale, and others. The thickness is 8.4 m.

Member 24 (Samples 2940/45–58) consists of dark gray and brown clays alternating with brown calcareous siltstones. The rocks contain ammonites *Riasanites crassicostatum* (Kvant. et Lys.), *Riasanites* sp., *Hegaratia taurica* (Bogd. et Kvant.), *H. bidichotoma* (Bogd. et Kvant.), and others and brachiopods *Loriolithyris valdensis* (Lor.), *Symphythiris arguinensis* (Moiss.), *Terebratuliopsis quadrata quadrata* Smirn., and other forms. In addition, ammonite *Faurella simplicostata* (Maz.) was found by B.T. Yanin in this member. The member under consideration contains also the impoverished foraminiferal *Triplasia emslandensis acuta* Assemblage dominated by agglutinated forms and ostracods represented by *Cytherella lubimovae* Neale, *C. fragilis* Neale, *Costacythere andreevi* Tes., and others. The thickness is 7.6 m.

Member 25 (sponge horizon, Samples 2940/59–65) in the outskirts of the Balki settlement is characterized by the following structure (from the base upward):

(1) Greenish gray unconsolidated clays (approximately 5 m) with abundant brachiopod *Symphythiris arguinensis* (Moiss.) remains, foraminifers of the *Triplasia emslandensis acuta* Assemblage dominated by *Lenticulina macra* Coup., *Spirillina kubleri* Mjatl. accompanied by single planktonic forms, spores of Schizaleales ferns *Cicatricosisporites* sp. and pollen of *Classopolllis* spp., dinocysts *Systematophora areolata* Klement and *Phallocysta elongata* (Beju), prasinophytes, and acritarchs.

(2) Light gray compact clotted limestones with abundant sponge skeletons, small oysters *Aetostreon subsinuatum* (Leym.), spines of echinoderms *Diplocidaris* (?) *bicarinata* Web., gastropods, and other organic remains such as brachiopods *Loriolithyris valdensis* (Lor.) and *Symphythiris arguinensis* (Moiss.), single ammonites *Riasanites crassicostatum* (Kvant. et. Lys.), and belemnite rostra. The limestones constitute isolated bioherms 1.0–1.5 m across submerged into the matrix of greenish clays. The thickness is at least 10–12 m.

(3) Alternating greenish gray clays and compact gray calcareous siltstones (4–6 m) crossed by abundant vertical *Ophiomorpha* and *Thalassinoides* burrows. The sediments contain single weathered pyrite concretions. The impoverished *Triplasia emslandensis acuta* foraminiferal assemblage is dominated by agglutinated forms accompanied by poorly preserved calcareous tests.

(4) Greenish gray unconsolidated clays (5 m) with ammonites *Hegaratia* sp. and *Spiticeras* sp. The *Lenticulina andromede* foraminiferal assemblage includes single specimens of planktonic forms.

Ostracods scattered through the entire sponge member are represented by the following species: *Cytherella krimensis* Neale, *C. lubimovae* Neale, *Cytherelloidea flexuosa* Neale, *Neocythere pyrena* Tes. et Rach. The integral thickness of the member is 28 m.

*Section 2943 (Mezhgor'e; 44°58′49.95″ N, 34°24′27.60″ E; Fig. 4)*

Samples 2943/1–5 were taken in the upper part of Member 25. The overlying sediments of Member 26 remained unsampled.

Member 26 (Samples 2943/6–13 were taken in the uppermost part of the member; samples for paleomagnetic measurements were taken from this member in 2002 in section 2420 near the Pasechnoe settlement located 600–700 m northeast of Section 2943) is composed of greenish gray unconsolidated clays and yellowish gray fine-grained sandy siltstones. Higher in the section, siltstones become progressively more calcareous to grade into marlstones. The member contains diverse organic remains: poorly preserved ammonites *Haploceras* ex gr. *cristifer* (Opp.), *Protetragonites tauricus* (Kulj.-Vor.), *Spiticeras* sp., and *Subalpinites* sp.; abundant bivalves *Gervillella* cf. *terekensis* (Renng.), *Entolium germanicum* (Woll.), *Chlamys goldfussi* (Desh.), *Neithea neocomiensis* (d'Orb.), *N. simplex* Mordv., *Plagiostoma dubisiensis* (Pict. et Camp.), *Ceratostreon minos* (Coq.), *Aetostreon subsinuatum* Leym., and others; brachiopods *Loriolithyris valdensis* (Lor.), *Terebratuliopsis quadrata quadrata* Smirn., *Weberithyris moisseevi* (Web.), and others; echinoderms *Acrocidaris minor* Ag., *Rhabdocidaris* aff. *burganensis* Web., and *Diplocidaris* (?) *bicarinata* Web.; crinoids *Apiocrinus* cf. *valangiensis* Lor. Sediments from the lower part of the member contain foraminifers of the *Lenticulina andromede* Assemblage; in its upper part, the latter is replaced by the *Conorboides hofkeri* Assemblage. Ostracods are represented by the following species: *Cytherelloidea mandelstami* Neale, *Bairdia menneri* Tes. et. Rach., *B. kuznetsovae* Tes. et. Rach., *Cypridea funduklensis* Tes. et Rach., *Eucytherura paula* Lueb., *Neocythere dispar* Donze, *Costacythere drushchitzi* (Neale), and others. There are also spores of Schizaleales ferns and other plants, *Classopollis* spp. pollen, dinocysts of the *Phoberocysta neocomica* Assemblage, prasinophytes, and acritarchs. The thickness is 30 m.

Member 27 (Samples 2943/14–15) consists of light gray and yellowish gray massive and slightly consolidated marlstones. Its upper part is characterized by diverse benthic macrofossils; corals; brachiopods *Terebratuliopsis quadrata quadrata* Smirn., *Weberithyris moisseevi* (Web.), *Zeillerina baksanensis* Smirn., and others; bivalves *Chlamys goldfussi* (Desh.), *Neithea atava* (Roem.), *N. neocomiensis* (d'Orb.), *Ceratostreon minos* (Coq.), and others; echinoderms *Rhabdocidaris* aff. *burganensis* Web. and *Pygopyrina incisa* (Ag.); and crinoids *A. neocomiensis* (d'Or.).

In 2002, E.Yu. Baraboshkin found in this member brachiopods *Loriolithyris valdensis* (Lor.), *Cyclothyris rectimarginata* Smirn., *Septaliphoria gerassimovi* Moiss., *Symphythiris koinautensis* (Moiss.), *Advenina villersensis* (Lor.), and other species.

The sediments contain also the impoverished foraminiferal association with *Textularia crimica* (Gorb.) and dominated by simple lituolids. The thickness is 15 m.

Member 28 (Samples 2943/16–20) is represented by light brown-gray compact clotted biohermal limestones with frequent accumulations of brachiopods *Zeillerina baksanensis* Smirn. and others in the lower part of the member, where they form coquinas, and abundant rudists in its upper part. Bioherms 1.5–2.0 m high are formed by corals, rudists, and algae and surrounded by organogenic–detrital and detrital limestones. The thickness is 25–30 m.

The Zeillerina baksanensis Beds are barren of guide ammonite species; therefore, many researchers considered them Valanginian (Drushchits and Yanin, 1959; Gorbachik et al., 1975). Subsequently, limestones were attributed to the Megadiceras koinautense Beds, which were dated back to the late Berriasian (Yanin and Baraboshkin, 2000).

The biohermal limestones of the Kuchki Formation near the Mezhgor'e settlement are overlain with the karst- and erosion-affected surface by quartz conglomerates (5–40 m), which may likely be considered as analogous to the Albat Member of the Bel'bek River basin, where it is, in turn, overlain by lower Valanginian strata (Yanin and Baraboshkin, 2000). Near the Mezhgor'e settlement, the surface of limestones is similarly uneven and bears indications of activity of borers. The conglomerates are overlain by a sandstone and clay sequence, which is overlain near the Balki settlement by oncolitic limestones with gastropods and rudists. In the opinion of T.N. Bogdanova in (Bogdanova et al., 1981), the conglomerates are replaced west of the Mezhgor'e settlement by white gastropod limestones, which are traceable up to the Petrovo settlement.

## BIOSTRATIGRAPHY

**Ammonites.** Of extreme interest is the finding of ammonite *Malbosiceras* ex gr. *malbosi* (Pictet) (Plate I) in the carbonate Bedenekyr Formation that underlies the terrigenous Bechku Formation in the outskirts of the Balki settlement (Section 2951). This ammonite was found in talus stratigraphically below the Malbosiceras chaperi Beds. The last unit defined by V.V. Arkadiev and T.N. Bogdanova in the Sary-Su River basin was correlated with the upper part of the jacobi Zone above the grandis Zone (Arkadiev et al., 2002, 2006). Previously, these sediments defined as the Malbosiceras (?) sp. Beds were attributed to the occitanica Zone (Bogdanova et al., 1981). Their correlation with any of these zones was ambiguous. V.V. Arkadiev identified from these beds *M. malbosi* (Pictet) together with *M. chaperi*. In Berriasian sections of Western Europe, the species *M. malbosi* is characteristic of the boissieri Zone (paramimounum Subzone), while *M. chaperi* occurs in the upper part of the jacobi Zone (Le Hégarat, 1973; Tavera, 1985). In Crimea, *M. malbosi* is, in addition, documented in the occitanica

Plate I

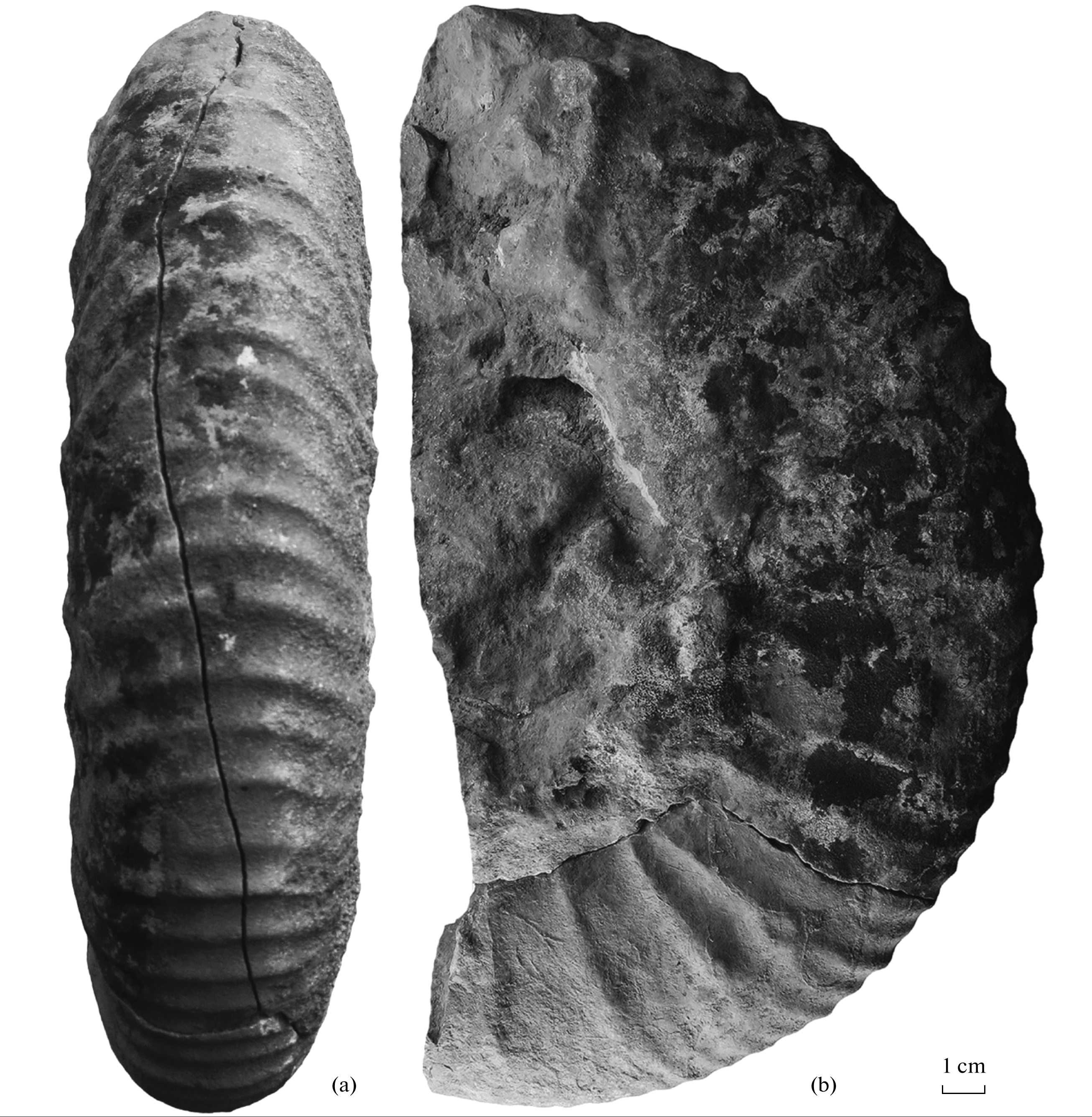


**Plate I.** *Malbosiceras* ex gr. *malbosi* (Pictet), specimen 1/13244.
(a) Ventral view (×0.7); (b) lateral view (×0.7); Balki settlement, Member 2, Berriasian, occitaniica Zone.

Zone (Arkadiev et al., 2012). Therefore, it is more reasonable to assume that it occurs at the lower level up to the jacobi Zone, not that *M. chaperi* continues occurring up to the occitanica Zone. In such a situation, the find of *Malbosiceras* ex gr. *malbosi* indirectly correlates the carbonate part of the examined section with the occitanica Zone. Magnetostratigraphic data, which register reverse polarity in outcrops 2950 and 2951 (Fig. 3), are consistent with correlation between the Malbosiceras chaperi Beds and occitanica Zone. In the paleomagnetic scale, Chron M17 corresponds to the upper part of the jacobi Zone and largest part of the occitanica Zone (Ogg and Hinnov, 2012).

**Bivalves.** The identified bivalve remains include both guide and marker species. In (Arkadiev et al., 2012), B.T. Yanin defined in the Berrisian Stage of Crimea three stratigraphic assemblages: lower–middle Berriasian, middle Berriasian, and upper Berriasian. *Neithea simplex* Mord. is a guide form for the lower assemblage. This species is characteristic of Berriasian strata of Kopetdag, Mangyshlak, and the northern Caucasus, in addition to the Crimean Mountains. *Prohinnites renevieri* (Coq.) occurs from the lower strata of the Berriasian Stage and characterizes its entire section in Crimea. *Entolium germanicum* (Woll.) is also characterized by a wide stratigraphic range occurring beyond the limits of the Berriasian Stage. At the same time, in Crimea this species appearing in the jacobi Zone forms peculiar coquinas in clayey sediments of the central Crimean Mountains; i.e., it represents a marker species for this part of the region under consideration. The species is less characteristic of the middle and upper parts of the Berriasian Stage, where it occurs as single specimens.

*Gervillella anceps* (Desh. in Leym.) and *Integricardium deshayesianum* (Lor.) are characteristic species of the upper middle Berriasian Dalmasiceras tauricum Subzone and largest part of the upper Berriasian. In sections of the Bel'bek River basin in southwestern Crimea, the first species (marker) forms coquinas. The second species is less frequent and never forms coquinas, being mostly distributed in the middle part of the Berriasian Stage in this area of the Crimean Mountains. *Tortarctica weberi* Mord. is also abundant in the same layers of the Berriasian section.

**Foraminifers.** These microfossils from Berriasian sediments of central Crimea (Plate II) were investigated in residues and thin sections using variably oriented sections. For samples from some levels, shells extracted from rocks were used for preparing polished sections. In total, foraminifers from the composite Berriasian sec-

**Plate II.** Foraminifers from Berriasian sediments of central Crimea. Magnification: ×20 for figs. 1–25, ×35 for figs. 26–49, ×60 for fig. 50.

(1) *Haplophragmium subaequale* (Mjatl.), specimen 27/1324: (1a) lateral view, (1b) peripheral view, (1c) polished thin section, Balki settlement, Member 18; (2, 3) *Charentia evoluta* Gorb: (2) specimen 31/1324: (2a) lateral view, (2b) peripheral view, Enisarai Ravine, Member 9; (3) specimen 32/1324, thin section, transverse section, Enisarai Ravine, Member 1; (4, 5) *Stomatostoecha compressa* Gorb.: (4) specimen 35/1324: (4a) lateral view, (4b) peripheral view, Enisarai Ravine, Member 9; (5) specimen 36/1324, thin section, transverse section, Enisarai Ravine, Member 1; (6–8) *Stomatostoecha enisalensis* Gorb.: (6) specimen 38/1324, thin section, transverse section, Balki settlement, Member 18; (7) specimen 39/1324, oblique section close to the longitudinal one, Enisarai Ravine, Member 1; (8) specimen 37/1324: (8a, 8b) lateral view, (8c) peripheral view, Enisarai Ravine, Member 11; (9, 10) *Melathrokerion spirialis* Gorb.: (9) specimen 33/1324: (9a, 9b) lateral view, (9c) peripheral view, Balki settlement, Member 18; (10) specimen 34/1324, thin section, transverse section, Enisarai Ravine, Member 1; (11) *Rectocylammina chouberti* Hott., specimen 48/1324: (11a) lateral view, (11b) apertural view, (11c) polished section, Enisarai Ravine, Member 5; (12) *Rectocylammina recta* Gorb., specimen 52/1324: (12a) lateral view, (12b) apertural view, (12c) polished section, Enisarai Ravine, Member 10; (13) *Rectocylammina arrabidensis* Remalho, specimen 46/1324: (13a) lateral view, (13b) apertural view, (13c) polished section, Enisarai Ravine, Member 11; (14, 16) *Everticyclammina virguliana* (Koechl.): (14) specimen 44/1324: (14a) lateral view, (14b) apertural view, (14c) polished section, Enisarai Ravine, Member 5; (16) specimen 42/1324, lateral view, Enisarai Ravine, Member 6; (15) *Everticyclammina elongata* Gorb., specimen 45/1324, polished section, Enisarai Ravine, Member 4; (17) *Alveosepta jaccardi* (Schrodt), specimen 62/1324: (17a, 17b) lateral view, (17c) peripheral view, Balki settlement, Member 18; (18) *Amijiella amiji* (Henson), specimen 54/1324, thin section, longitudinal section, Enisarai Ravine, Member 4; (19) *Bramkampella arabica* Radm., specimen 55/1324, thin section, longitudinal section, Enisarai Ravine, Member 11; (20, 21) *Textularia crimica* (Gorb.), specimen 56/1324: (20a) lateral view, (20b) apertural view, Mezhgor'e settlement, Member 26; (21) specimen 57/1324, thin section, longitudinal section, ibid; (22–24) *Belorussiella taurica* Gorb.: (22) specimen 58/1324, lateral view, Mezhgor'e Settlement, Member 26; (23) specimen 59/1324, thin section, ibid; (24) specimen 60/1324, thin section, ibid; (25) *Triplasia emslandensis acuta* Brat. et Brand, specimen 30/1324: (25a, 25b) lateral view, (25c) apertural view, Balki settlement, Member 21; (26) *Lenticulina ongkodes* Esp. et Sigal, specimen 66/13244, Balki settlement, Member 21; (27) *Lenticuina aquilonica* Mjatl., specimen 67/13244: (27a) lateral view, (27b) peripheral view, Enisarai Ravine, Member 15; (28) *Lenticulina* aff. *uspenskajae* K. Kuzn., specimen 68/13244: (28a) lateral view, (28b) peripheral view, Enisarai Ravine, Member 15; (29) *Lenticulina muensteri* (Roemer), specimen 63/13244: (29a) lateral view, (29b) peripheral view, Mezhgor'e settlement, Member 26; (30) *Lenticulina andromede* Esp. et. Sigal, specimen 64/13244: (30a) lateral view, (30b) peripheral view, Mezhgor'e settlement, Member 26; (31) *Lenticulina colligoni* Esp. et Sigal, specimen 65/13244: (31a) lateral view, (31b) peripheral view, Enisarai Ravine, Member 15; (32) *Lenticulina bifurcata* Bart. et Brand, specimen 69/13244: (32a) lateral view, (32b) peripheral view, Enisarai Ravine, Member 15; (33) *Lenticulina* sp. (*L.* sp. 1 Gorb.), specimen 80/13244: (33a) lateral view, (33b) peripheral view, Balki settlement, Member 21; (34) *Lenticulina macra* Gorb., specimen 70/13244: (34a) lateral view, (34b) peripheral view, Enisarai Ravine, Member 13; (35) *Lenticulina fracta* Esp. et Sigal, specimen 73/13244: (35a) lateral view, (35b) peripheral view, Enisarai Ravine, Member 13; (36, 37) *Lenticulina ambanjabensis* (Esp. et Sigal): (36) specimen 77/13244: (36a) lateral view, (36b) peripheral view, Mezhgor'e settlement, Member 26; (37) specimen 78/13244, thin section close to the orthogonal one, Enisarai Ravine, below Member 1; (38) *Lenticulina eichenbergi* Bart. et Brand, specimen 82/13244: (38a) lateral view, (38b) peripheral view, Mezhgor'e settlement, Member 26; (39) *Lenticulina neocomina* Rom., specimen 74/13244: (39a) lateral view, (39b) peripheral view, Mezhgor'e settlement, Member 26; (40) *Astacolus mutilatus* Esp. et Sigal, specimen 84/13244, Balki settlement, Member 18; (41) *Astacolus proprius* K. Kuzn., specimen 85/13244, Balki settlement, Member 18; (42) *Astacolus folium* (Wisn.), specimen 86/13244, Balki settlement, Member 18; (43) *Saracenaria latruncula* (Chalilov), specimen 87/13244, Balki settlement, Member 21; (44) *Saracenaria inflata* Pathy, specimen 90/13244: (44a) lateral view, (44b) peripheral view, Mezhgor'e settlement, Member 26; (45) *Saracenaria aculata* Esp. et Sigal, specimen 89/13244: (45a) lateral view, (45b) peripheral view, Enisarai Ravine, Member 15; (46) *Saracenaria compacta* (Esp. et Sigal), specimen 91/13244: (46a) lateral view, (46b) peripheral view, Enisarai Ravine, Member 15; (47) *Saracenaria tsarmandrosoensis* Esp. et Sigal, specimen 93/13244, Mezhgor'e settlement, Member 26; (48) *Saracenaria provoslavlevi* Furs. et Pol., specimen 94/13244: (48a) lateral view, (48b) peripheral view, Enisarai Ravine, Member 13; (49) *Pseudosaracenaria truncata* Pathy, specimen 92/13244, Balki settlement, Member 21; (50) *Conorboides hofkeri* (Bart. et Brand), specimen 111/13244: (50a) dorsal view, (50b) ventral view, (50c) peripheral view, Mezhgor'e settlement, Member 26.

Plate II

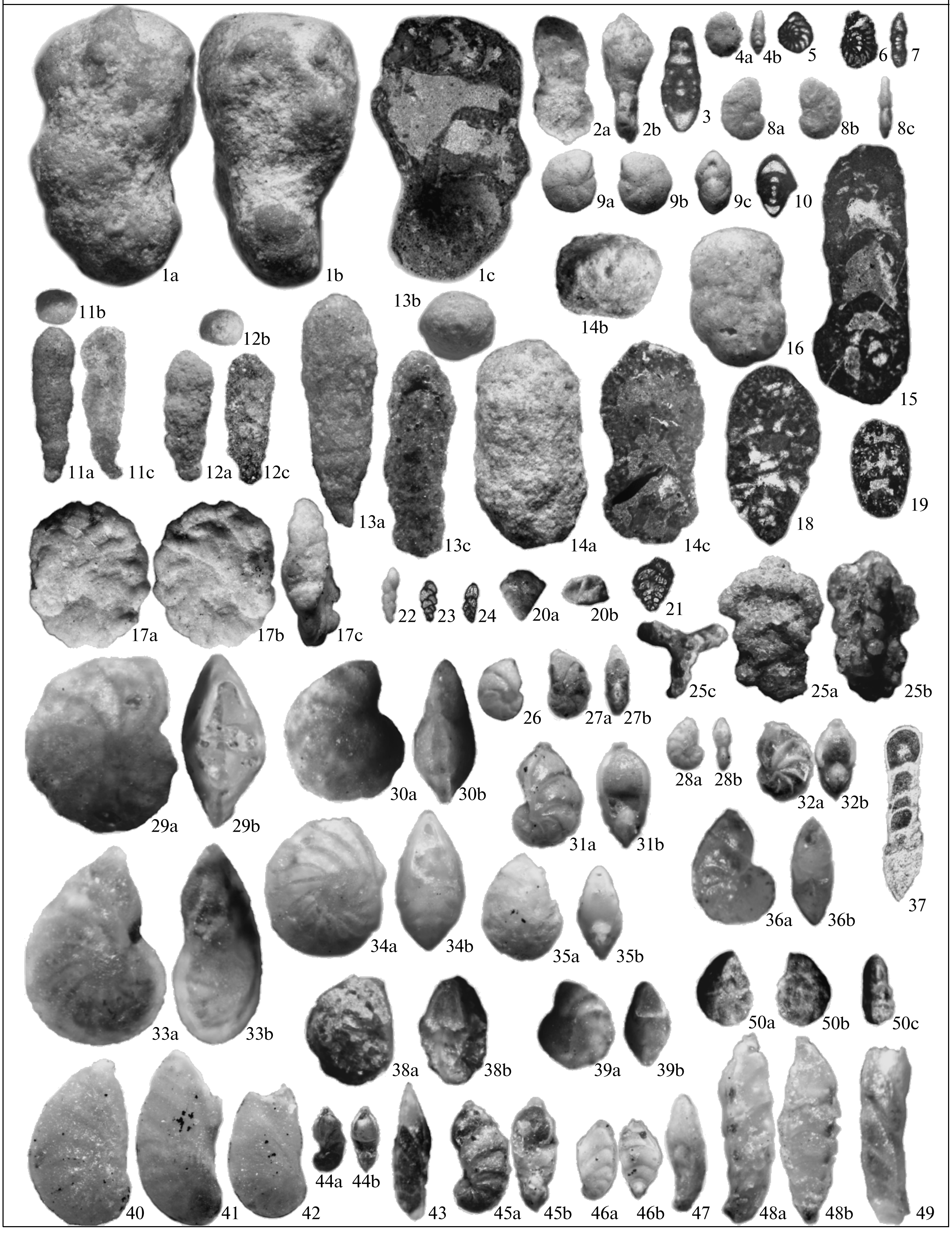
1a
1b
1c
2a
2b
3
4a
4b
5
6
7
8a
8b
8c
9a
9b
9c
10
11a
11b
11c
12a
12b
12c
13a
13b
13c
14a
14b
14c
15
16
17a
17b
17c
18
19
20a
20b
21
22
23
24
25a
25b
25c
26
27a
27b
28a
28b
29a
29b
30a
30b
31a
31b
32a
32b
33a
33b
34a
34b
35a
35b
36a
36b
37
38a
38b
39a
39b
40
41
42
43
44a
44b
45a
45b
46a
46b
47
48a
48b
49
50a
50b
50c

tion are represented by over 200 species of 63 genera (Fig. 5). As a whole, the identified foraminiferal assemblage is characteristic of the Textularia crimica–Belorussiella taurica Beds developed through the entire Crimean Region (Feodorova, 2004). The following six successive foraminiferal assemblages may be defined in the section under consideration on the basis of changes in the taxonomic composition and quantitative parameters (from the base upward) (Fig. 5):

1. *The Everticyclammina virguliana–Retrocyclammina recta–Bramkampella arabica* Assemblage (Members 1–12 and 18). This assemblage is characterized by the prevalence of lituolids (including complex) over nodosariid. The assemblage numbers 70 species of 45 genera in total. The characteristic species are abundant and diverse representatives of the genera *Everticyclammina* and *Retrocyclammina*, including *Retrocyclammina* ex gr. *chouberti* Hott, *R. recta* Gorb., *Everticyclammina virguliana* (Koechl.), and *E. elongata* Gorb., as well as *Haplophragmium subaequale* (Mjatluk), *Melathrokerion spirialis* Gorb., *Charentia evoluta* (Gorb.), *Pseudocyclammina lituus* (Yok.), *Stomatostoecha rotunda* Gorb., *S. compressa* Gorb., *S. enisalensis* Gorb., *Bramkapella arabica* Radm., *Amijella amiji* (Henson), *Belorussiella taurica* Gorb., *Alveosepta jaccardi* (Schrodt), *Astacolus mulitatus* Esp. et Sigal, *A. inspissatus* (Loeblich et Tappan), *A. favoritus* Gorb., *Discorbis miser* Gorb., *Trocholina alpina* (Leup.), *T. elongata* (Leup.), *T. molesta* Gorb., *T. infragranulata* Noth, and others. Thin sections from the lower part of the section (Member 2) yielded single specimens of *Protopeneroplis ultragranulatus* (Gorb.) and *Pseudosiphoninella antiqua* (Gorb.). The assemblage is named after species *E. virguliana, R. recta*, and *B. arabica*.

The Rectocyclammina Beds transitional from the upper Tithonian to lower Berriasian, which are established on the Ai-Petri Plateau, and the Bramkapella Beds from the overlying limestone sequence (Gorbachik and Mokhamad, 1999) are characterized by a similar foraminiferal assemblage. The Bramkapella Beds are taken by the last authors to be the early Berriasian in age.

It should be noted that the *Everticyclammina virguliana–Retrocyclammina recta–Bramkampella arabica* Assemblage is registered also in Member 18, which is located higher in the section. The assemblage from this member is characterized by the presence of many (several hundred) specimens of *Melathrokerion spirialis* Gorb. and species *Flabellammina lidiae* Gerke et Pol. and *Triplasia elegans* (Mjatl.), which are known from terminal Jurassic strata of the Boreal and Arctic provinces, against the background of dominant complex Lituolidae. These data combined with petromagnetic measurements may presumably indicate that Member 18 is repeated in the section, although this assumption requires additional investigations. We leave Member 18 in the general stratigraphic succession, although with the question mark.

2. *The Lenticulina muensteri* Assemblage (Members 13–17, 19) is notably dominated by Nodosariidae with representatives of the genera *Lenticulina* being particularly abundant and diverse and genera *Saracenaria* and *Pseudonodosaria* being subdominant. The assemblage is named after the characteristic species, which is present in all the examined samples. In total, the assemblage includes approximately 65 species of 22 genera with *Ramulna aculeata* Wright, *Lenticulina nimbifera* Esp. et Sigal, *L. fracta* Esp. et Sigal, *Pseudonodosaria diversa* (Hoff.), *Saracenaria compacta* Esp. et Sigal, and *Hoeglundina* ex gr. *caracolla* (Roemer) being dominant. The following species are also characteristic: *Dorothia* ex. *oxycona* (Reuss), *D. kummi* Zedler (minima), *Nodosaria raristriata* Chapman, *Tristix acutangulus* (Reuss), *Lenticulina muensteri* (Roemer), *L. colligoni* Esp. et Sigal, *Astacolus proprius* Kun., *A. incurvatus* (Reuss), *Marginulina striatocostata* Reuss, *M. micra* Tairov, *Marginulinopsis sigali* Bart., Bett. et Bolli, *Saracenaria provoslavlevi* Furs. et Pol., *S. provoslavlevi* Furs. et Pol. var. *minima*, *S. aculata* Esp. et Sigal, *Dentalina gracilis* d'Orb., *D. guttinfera* d'Orb., *Citharinella pectinatimornata* Esp. et Sigal, *Trocholina micra* Dulub., and others. The characteristic feature of this assemblage is alternative development of normal, dwarfish, and giant forms.

3. *The Quadratina tunassica* Assemblage (Member 20) is the least representative one, consisting only of approximately 30 species belonging to 23 genera. The assemblage is characterized by gigantism among simple lituolids. It is named after the index species of the Quadratina tunassica–Siphonella antiqua Zone (Drushchits and Gorbachik, 1979), which corresponds approximately to the upper part of the grandis Zone and lower part of the occitanica Zone. It is defined on the basis of the appearance of *Quadratina tunassica* Schokhina and *Lenticulina protodecimae* Dieni et Massari and the presence of single transit species such as *Textularia crimica* (Gorb.), *T. densa* Hoff., *Citharinella pectinatimornata* Esp. et Sigal, *Citharina flexuosa* (Bruck.), *Tristix acutangulus* (Reuss), *Lenticulina colligoni* Esp. et Sigal, *L. muensteri* (Roemer), *Astacolus incurvatus* (Reuss), *Nodosaria paupercula* Reuss, *Saracenaria latruncula* (Chalilov), *Planularia crepidiularis* Roemer, *Lagena sztejnae* Dieni et Massari, and *Spirillina kubleri* Mjatl.

4. *The Triplasia emslandensis acuta* Assemblage (Members 21–24 and lower part of Member 25) is distributed discretely through the section. In total, the assemblage includes over 100 species of 47 genera, among which *Lenticulina* representatives are dominant and species of the genera *Saracenaria* and *Verneuilina* are subdominant. It is named after the index species of the synonymous Triplasia emslandensis acuta Subzone (Kuznetsova and Gorbachik, 1985), approximately correlated with the upper part of the occitanica Zone and lower part of the boissieri Zone.

The assemblage is defined on the basis of the appearance of *Recurvoides* ex gr. *paucus* Dubr., *Haplophragmoides subchapmani* K. Kuzn., *Triplasia emslan-*

*densis acuta* Brat. et Brand., *Pseudolamarckina reussi* (Ant.), *Lenticulina nuda* (Reuss), *L. nodosa* (Reuss), and *Saracenaria inflata* Pathy and the presence of abundant specimens of transit species: *Lenticulina macra* Gorb., *L. neocomina* Rom., *Vaginulina kochii* Roemer, *Saracenaria latruncula* (Chalilov), *Spirillina kubleri* Mjatl.

5. *The Lenticulina andromede* Assemblage (upper part of Member 25 and lower part of Member 26) is represented by over 70 species of 40 genera with the distinctly dominant share of *Lenticulina* representatives. The assemblage is marked by the appearance of abundant *Lenticulina andromede* Esp. et Sigal, *Tristix valanginica* Schokhina, *Lenticulina guttata guttata* (Dam), *L.* ex gr. *ouachensis* Sigal, *L. praegaultina* Bart., *Falsopalmula costata* Gorb., and *Istriloculina rectoangularia* Mats. et Temirb. They are accompanied by species inherited from underlying sediments: abundant *Ramulina aculeata* Wright, *Ammobaculites inconstans gracilis* Bart. et Brand, *Textularia crimica* (Gorb.), *Belorussiella taurica* Gorb., *Lenticulina nuda* (Reuss), *L. macra* Gorb., *L. neocomina* Rom., *Discorbis praelongus* Gorb., *Spirillina kubleri* Mjatl., and others.

6. *The Conorboides hofkeri* Assemblage (upper part of Member 26) is named after one of the index species of the Conorbina heteromorpha–Conorboides hofkeri Zone (Drushchits and Gorbachik, 1979), correlated with the upper part of the occitanica Zone and boissieri Zone.

The assemblage includes over 50 species of 30 genera being barren of distinct dominant forms. It is marked by the appearance of *Dorothia kummi* Zedler, *Dentalina marginulinoides* Reuss, *Miliospirella caucasica* Ant., *Discorbis agalarovae* Ant., *Epistomina tenuicostata* Bart. et Brand, *E. ornata* (Roemer), and *Conorboides hoffkeri* (Bart. et Brand), accompanied by abundant transit species *Belorussiella taurica* Gorb., *Pseudolamarckina reussi* (Ant.), *Saracenaria inflata* Pathy, *Hoeglundina* ex gr. *caracolla* (Roemer), and *Spirillina kubleri* Mjatl. and common *Bulbabaculites inconstans* (Bart. et Brand), *Nautiloculina oolithica* Mochler, *Textularia crimica* (Gorb.), *Lenticulina macra* Gorb., *L. muensteri* (Roemer), *Astacolus ambanjabensis* (Esp. et Sigal), *Trocholina giganta* Gorb. et Manz., and others.

In central Crimea, Berriasian foraminifers were investigated by T.N. Gorbachik (Kuznetsova and Gorbachik, 1985). The comparison of our data with the results of this author is difficult since she mentions only 31 species for the entire Berriasian section of central Crimea, including taxa identified with the open nomenclature.

The foraminiferal species documented in the examined sections are known from the Tithonian–Valanginian sections of Crimea, the Caucasus, the Caspian region, Syria, Germany, France, Italy, and Madagascar. Within the Tethyan region, the *Everticyclammina virguliana–Retrocyclammina recta–Bramkampella arabica* Assemblage of central Crimea is most similar to Berriasian foraminiferal assemblages of Syria, the northern Caspian region, southeastern France, and Italy. The assemblages from the middle and upper parts of Berriasian sections in central Crimea are best comparable with their counterparts from the "Cenozone D" of Madagascar (Espitalie and Sigal, 1963).

Thus, the foraminiferal assemblages allow successful subdivision and correlation of sections within particular regions, while their potential in interregional correlations without ammonites is very low.

**Ostracods.** The discovery of previously unknown parts of the Berriasian section in central Crimea in 2012 substantially widened the range and characteristics of the previously defined Costacythere khiamii–Hechticythere belbekensis Beds (Arkadiev et al., 2012). The identified ostracod remains belong to 16 families. Their assemblage includes 85 species of 33 genera in total. The core of their assemblages is represented by smooth-walled forms characterized by a wide facies and stratigraphic distribution (*Cytherella*) and abundant representatives of the tropical (subtropical) genus *Cytherelloidea*. Of interest is the presence of brackish- and freshwater genus *Cypridea*, which is characterized by rare specimens. Ornamented forms are mostly represented by genera of the families Protocytheridae (*Protocythere, Reticyhere, Hechticythere, Costacythere*) and Cytheruridae (*Eucytherura*) (Plate III).

The taxonomic and quantitative analyses of ostracod assemblages allow two biostratigraphic units of the beds rank to be defined in the examined Berriasian section (Fig. 6). The lower part of the section conditionally correlated with the ammonite occitanica Zone contains 45 ostracod species belonging to 24 genera. It is united into the Costacythere khiamii–Hechticythere belbekensis Beds on the basis of the co-occurrence of characteristic species and high abundance of *Costacythere khiamii* specimens.

The ostracod assemblage from the upper part of the section corresponding to the part of the ammonite boissieri Zone numbers 71 species of 28 genera. It is characterized by the dominant role of the genera *Cytherella, Cytherelloidea, Paracypris, Costacythere*, and *Reticythere*. Many species are inherited from underlying sediments (36 species of 20 genera in common), while others appear at this level for the first time (35 species of 22 genera). This part of the section is attributed to the Costacythere drushchitzi–Reticythere marfenini Beds on the basis of high abundance and joint occurrence of these characteristic species.

The ostracod species registered in the examined section are mostly known from Lower Cretaceous (Berriasian–Hauterivian) deposits of Crimea (Neale, 1966; Tesakova and Rachenskaya, 1996a, 1996b), the North Caucasus (Kolpenskaya, 2000), Central Asia (Andreev, 1986), England (Neale, 1962, 1967, 1978; Slipper, 2009), France (*Atlas*..., 1985; Donze, 1964, 1965; etc.), Germany (Triebel, 1938; Gründel, 1964; etc.), and Poland (Kubiatowicz, 1983). *Acrocythere diversa* Donze and *Bythoceratina variabilis* Donze are first described from Berriasian strata of France (Donze,

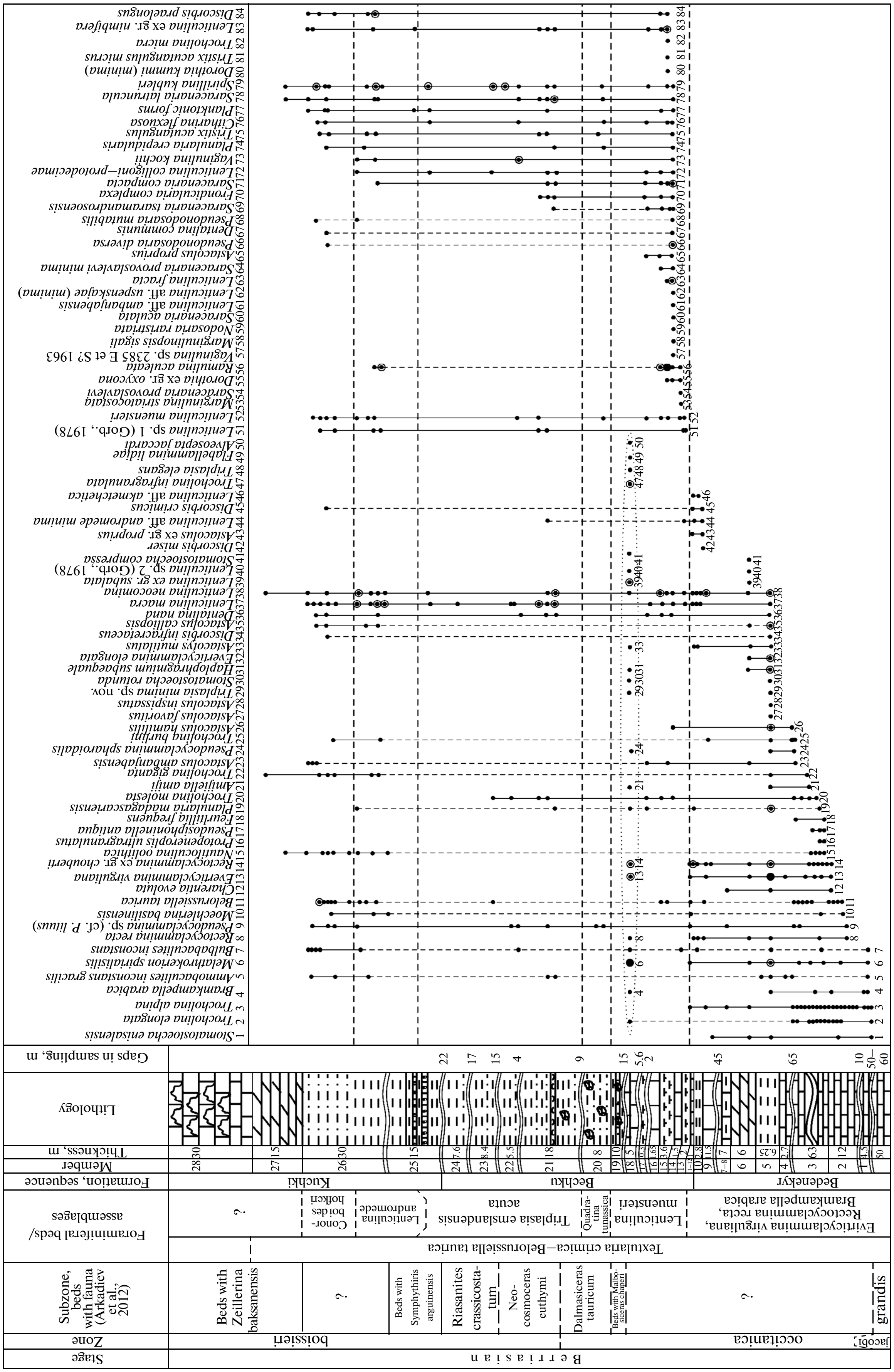


**Fig. 5.** Stratigraphic distribution of main foraminiferal species in Berriasian sections of central Crimea. For legend, see Fig. 4.

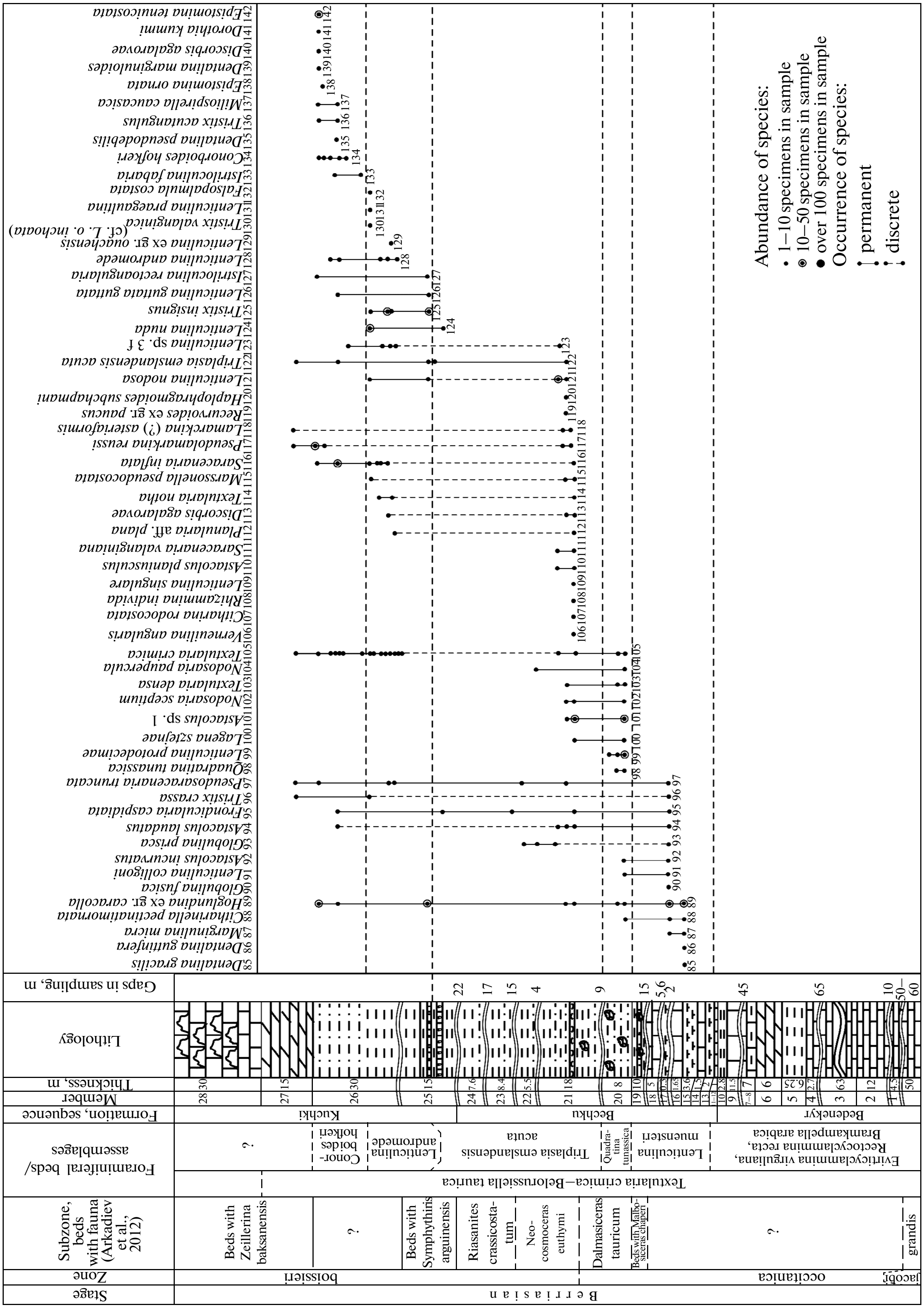
Stage
Zone
Subzone, beds with fauna (Arkadiev et al., 2012)
Foraminiferal beds/assemblages
Formation, sequence
Member
Thickness, m
Lithology
Gaps in sampling, m
Berriasian
jacobi
occitanica
boissieri
grandis
Beds with Malbosiceras chaperi
Dalmasiceras tauricum
Neocosmoceras euthymi
Riasanites crassicostatum
Beds with Symphythiris arguinensis
Beds with Zeillerina baksanensis
Textularia crimica–Belorussiella taurica
Evirticyclammina virguliana, Rectocyclammina recta, Bramkampella arabica
Lenticulina muensteri
Quadratina tunassica
Triplasia emslandensis acuta
Lenticulina andromede
Conorboides hofkeri
Bedenekyr
Bechku
Kuchki
Dentalina gracilis
Dentalina guttifera
Marginulina micra
Citharinella pectinatimorniata
Hoglundina ex gr. caracolla
Globulina fusica
Lenticulina collignoni
Astacolus incurvatus
Globulina prisca
Astacolus laudatus
Frondicularia caspidiata
Tristix crassa
Pseudosaracenaria truncata
Quadratina tunassica
Lenticulina protodecimae
Lagena szteinae
Astacolus sp. 1
Nodosaria sceptrum
Textularia densa
Nodosaria paupercula
Textularia crimica
Verneuilina angularis
Citharina rodocostata
Rhizammina individa
Lenticulina singulare
Astacolus planiusculus
Saracenaria valanginiana
Planularia aff. plana
Discorbis agalarovae
Textularia notha
Marssonella pseudocostata
Saracenaria inflata
Pseudolamarckina reussi
Lamarckina (?) asteriaformis
Recurvoides ex gr. paucus
Haplophragmoides subchapmani
Lenticulina nodosa
Triplasia emslandensis acuta
Lenticulina sp. 3 f
Lenticulina nuda
Tristix insignus
Lenticulina guttata guttata
Istriloculina rectangularia
Lenticulina andromede
Lenticulina ex gr. ouachensis (cf. L. o. inchoata)
Tristix valanginica
Lenticulina praegaultina
Falsopalmula costata
Istriloculina fabaria
Conorboides hofkeri
Dentalina pseudodebilis
Tristix acutangulus
Miliospirella caucasica
Epistomina ornata
Dentalina marginuloides
Discorbis agalarovae
Dorothia kummi
Epistomina tenuicostata
Abundance of species:
1–10 specimens in sample
10–50 specimens in sample
over 100 specimens in sample
Occurrence of species:
permanent
discrete

**Fig. 5.** (Contd.)

1964). *Metacytheropteron* sp. A Pok., *Quasigermanites bicarinatus moravicus* Pok., *Eucytherura trinodosa* Pok., and two close species *Eucytherura* ex gr. *trinodosa* Pok. and *Eucytherura* aff. *soror* Pok. are identified in Tithonian sections of the Czech Republic (Pokorny, 1973). Of these species, *E. trinodosa, E.* ex gr. *trinodosa*, and *E.* aff. *soror* were found in the upper Tithonian–lower Berriasian section of eastern Crimea (Arkadiev et al., 2012). The subspecies *Quasigermanites bicarinatus moravicus* Pok. was previously recorded in the upper part of the Berriasian section of eastern Crimea, while the close species *Quasigermanites* aff. *bicarinatus* Pok. was documented in the middle part of the Berriasian section in southwestern Crimea. *Neocythere dispar* Donze was first described from the basal part of the Valanginian Stage in the stratotype region of the Berriasian Stage (Donze, 1965) and subsequently registered in Berriasian layers of Mangyshlak (Andreev and Oertli, 1970). We found this species in the upper and middle–upper parts of the Berriasian section in the central and western parts of the Crimean Peninsula, respectively. Many ostracod species were first described from the Berriasian section of central Crimea: *Cytherella krimensis* Neale, *C. lubimovae* Neale, *Cytherelloidea flexuosa* Neale, *C. mandelstami* Neale, *Bairdia menneri* Tes. et Rach., *B. kuznetsovae* Tes. et Rach., *Cypridea funduklensis* Tes. et Rach., *Pontocyprella nova* Neale, *Pontocypris cuneata* Neale, *Neocythere pyrena* Tes. et Rach., *Costacythere khiamii* Tes. et Rach., *C. drushchitzi* (Neale), *C. andreevi* Tes. et Rach., *C. foveata* Tes. et Rach., *Hechticythere belbekensis* Tes. et Rach., *Reticythere marfenini* (Tes. et Rach.), *Eocytheropteron* sp. A Neale (Neale, 1966; Tesakova and Rachenskaya, 1996a, 1996b).

The defined ostracod assemblages of central Crimea exhibit the most similarity to their assemblage from the Berriasian stratotype (13 genera and 2 species in common) (Grekoff and Magne, 1966; Neale, 1967). The similarity at the species level is noted to the Berriasian assemblage from the section cropping out along the Urukh River in the North Caucasus (10 genera and 7 species in common) (Kolpenskaya, 2000). Nevertheless, a reliable correlation between ostracod beds defined in central Crimea and coeval stratigraphic units in the Urukh section is impossible. The assemblage of the Costacythere khiamii– Hechticythere belbekensis Beds is comparable with the similar Berriasian assemblage from the Berriasian tauricum Subzone defined in southwestern Crimea (Bel'bek River basin) (Arkadiev et al., 2012).

It should be noted that the ostracod assemblage from the upper part of Section 2952 (Sample 49-9-1) is similar in its taxonomic composition and abundance of *Cytherella lubimovae*, *Costacythere khiamii*, and *C. foveata* to the assemblage from Section 2949 (Sample 39-2-1).

**Palynomorphs.** In total, 28 samples were subjected to the palynological analysis.

The samples were treated in accordance with the traditional technique used in palynological investigations, which is based on the hydrofluoric method and modified technology (Raevskaya and Shurekova, 2011). No palynomorphs are observed in 12 samples. Other samples contain variable quantities of spores, pollen, and microphytoplankton represented by well-preserved cysts of dinoflagellates, prasinophytes, and acritarchs (Plate IV).

The proportions of palynomorphs in different parts of the section are variable. In the lower part of the ammonite Dalmasiceras tauricum Subzone, the palynomorph assemblage is represented by *Classopollis* pollen (47%), spores and bisaccate coniferous pollen (1%), and marine microphytoplankton (52%). In the remaining part of the section, *Classopollis* pollen constitutes up to 90% and spores + bisaccate coniferous pollen are 1–5%. The share of microphytoplankton varies from 15% in the Malbosiceras chaperi Beds to

**Plate III.** Ostracods from Berriasian sediments of central Crimea.

(1) *Cytherella krimensis* Neale, specimen 2/13244, left valve, lateral view, Balki settlement, occitanica Zone; (2) *Cytherella lubimovae* Neale, specimen 176/13220, left valve, lateral view, Balki settlement, boissieri Zone, Symphythris arguinensis Beds; (3) *Paracypris felix* (Neale), specimen 3/13244, left lateral view, Balki settlement, occitanica Zone; (4) *Cytherelloidea flexuosa* Neale, specimen 4/13244, left valve, lateral view, Balki settlement, occitanica Zone; (5) *Cytherelloidea mandelstami* Neale, specimen 5/13244, left valve, lateral view, Balki settlement, occitanica Zone; (6) *Eucytherura* ex gr. *trinodosa* Pokorny, specimen 6/13244, left valve, lateral view, Balki settlement, occitanica Zone; (7) *Eucytherura* sp. 1, specimen 7/13244, right valve, lateral view, Balki settlement, occitanica Zone; (8) *Eucytherura* sp., specimen 8/13244, left valve, lateral view, Balki settlement, occitanica Zone; (9) *Paranotacythere* sp., specimen 9/13244, left valve, lateral view, Balki settlement, occitanica Zone; (10) *Eocytheroteron* sp., specimen 10/13244, left valve, lateral view, Balki settlement, occitanica Zone; (11) ?*Furbergiella* sp., specimen 11/13244, left valve, lateral view, Balki settlement, occitanica Zone; (12) *Neocythere pyrena* Tes. et Rach., specimen 212/13220, left valve, lateral view, Balki settlement, bossieri Zone, euthymi Subzone; (13) *Costacythere drushchitzi* (Neale), specimen 230/13220, right valve, lateral view, male, Mezhgor'e settlement, bossieri Zone; (14) *Costacythere drushchitzi* (Neale), specimen 12/13244, right lateral view, Balki settlement, occitanica Zone; (15) *Reticythere marfenini* Tes. et Rach., specimen 13/13244, left lateral view, male, Balki settlement, bossieri Zone, euthymi Subzone; (16–18) *Costacythere khiami* Tes. et Rach.: (16) specimen 14/13244; (17) specimen 15/13244, left lateral views; (18) specimen 16/13244, right valve, lateral view, females, Balki settlement, occitanica Zone; (19, 20) *Costacythere foveata* Tes. et Rach.: (19) specimen 17/13244, left valve, lateral view, female; (20) specimen 18/13244, left valve, lateral view, male, Balki settlement, occitanica Zone; (21) *Costacythere andreevi* Tes. et Rach., specimen 19.13244, left valve, lateral view, Balki settlement, occitanica Zone; (22) *Hechticythere belbekensis* Tes. et Rach., specimen 20.13244, right valve, lateral view, Balki settlement, occitanica Zone, tauricum Subzone; (23) *Cythereis* sp. B, specimen 21/13244, right valve, lateral view, Balki settlement, occitanica Zone; (24) *Schuleridea* ex gr. *juddi* Neale, specimen 22/13244, right lateral view, Balki settlement, occitanica Zone.

Plate III

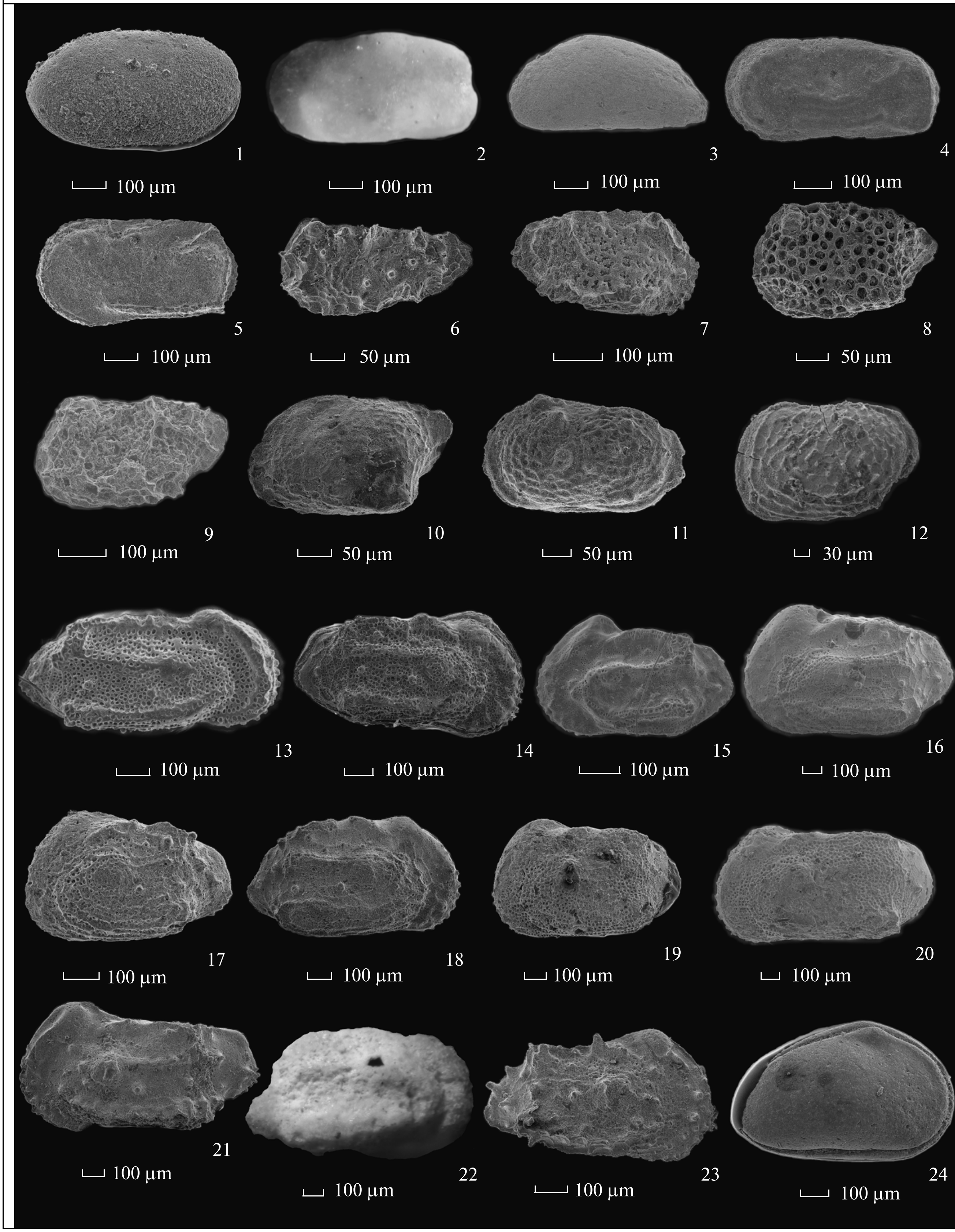
1
100 μm
2
100 μm
3
100 μm
4
100 μm
5
100 μm
6
50 μm
7
100 μm
8
50 μm
9
100 μm
10
50 μm
11
50 μm
12
30 μm
13
100 μm
14
100 μm
15
100 μm
16
100 μm
17
100 μm
18
100 μm
19
100 μm
20
100 μm
21
100 μm
22
100 μm
23
100 μm
24
100 μm

5% in the upper part of the ammonite tauricum Subzone and boissieri Zone.

Through the entire section (Fig. 7), spores are represented by smooth grains of *Leiotriletes* spp., *Cyathidites* sp., and Schizaleales ferns with the costate (*Cicatricososporites* sp.), grumous (*Verrucosisporites* sp.), and foveate (*Klukisporites variegatus* Coup.) exine. The sediments of the Dalmasiceras tauricum Subzone and boissieri Zone are marked by the appearance of Pteropsida spores *Eboracia torosa* (Sach. et Iljina), *Concavissimisporites punctatus* (Delcourt et Sprumont), *Kraeuselisporites* sp., and *Microlepidites crassirimosus* Timosch. and spores of Gleicheniaceae and Lycopodiaceae ferns (*Lycopodiumsporites* sp., *Densiosporites velatus* Weyland et Krieger).

The pollen spectrum includes grains of *Classopollis* spp., *Piceapollenites* spp., *Pinuspollenites* spp., *Callialasporites dampieri* (Balme), and *Quadraeculina anellaeformis* Mal.

The *Phoberocysta neocomica* dinocyst assemblage defined in the interval of the Berriasian section most saturated with marine phytoplankton remains (lower part of the ammonite Dalmasiceras tauricum Subzone) is represented by the following groups:

(1) chorate and proximoshorate cysts of dinoflagellates: *Hystrichosphaerina*? *orbifera* (Klement), *Systematophora areolata* Klement, *Kleithriasphaeridium eoinodes* (Eisenack), *Tanyosphaeridium isocalamum* (Deflandre et Cookson), *Dichadogonyaulax*? *pannea* (Norris), *Dichadogonyaulax culmula* (Norris), *Achomosphaera* sp., *Cleistosphaeridium varispinosum* (Sarjent), *Ctenidodinium* sp., *Epiplosphaera reticulospinosa* Klement, *Bourkidinium* sp., *Sentusidinium* spp.;

(2) cavate cysts of dinoflagellates: *Scriniodinium campanula* Gocht, *Gonyaulacysta* sp., *Phoberocysta neocomica* (Gocht);

(3) proximate cysts of dinoflagellates: *Pseudoceratium* cf. *pelliferum* Gocht, *Apteodinium* sp., *Rhynchodiniopsis martonensis* Bailey et al., *Rh. cladophora* (Deflandre), *Cribroperidinium* sp., *Nannoceratopsis deflandrei* Evitt subsp. *deflandrei*, *Durotrigia* sp.;

(4) prasinophytes of the genus *Pterospermella*;

(5) acritarchs *Micrhystridium* sp.

In the upper part of the ammonite Dalmasiceras tauricum Subzone and in the boissieri Zone, microphytoplankton is represented by cysts of the dinoflagellate species *Systematophora areolata* Klement, *Epiplosphaera* spp., *Kleithriasphaeridium eoinodes* (Eisenack), *Phoberocysta neocomica* (Gocht), *Rhynchodiniopsis cladophora* (Deflandre), *Durotrigia* sp., and *Oligosphaeridium patulum* Riding et Thomas; prasinophytes belonging to the genus *Pterospermella*; and diverse acritarchs. Despite the scarcity of the taxonomic composition of microphytoplankton remains in this interval of the section, it contains species characteristic of the above-mentioned *Phoberocysta neocomica* dinocyst assemblage from the lower part of the Dalmasiceras tauricum Subzone. The impoverishment of the assemblage is most likely explained by changes in depositional environments.

The Phoberocysta neocomica Beds established in central Crimea are also recognizable in southwestern and eastern parts of the peninsula (Arkadiev et al., 2012). The dinocyst assemblage from this unit is correlated with the assemblage from the Berriasian Dichadogonyaulax bensoni dinocyst zone of France (Monteil, 1992), upper Riazanian–lower Valanginian Pheoberocysta neocomica Zone of northwestern Europe (Fisher and Riley, 1980), and synonymous dinocyst zone of eastern Canada (Williams, 1975).

The microphytoplankton assemblage documented in the Malbosiceras chaperi Beds and underlying strata (Sections 2949, 2948) includes the following groups: proximate cysts of dinoflagelaltes species *Batiacasphaera* sp., *Cribroperidinium* sp., *Muderongia simplex* Alberti, and *Muderongia* Complex; chorate and proximate cysts *Kleithriasphaeridium eoinodes* (Eisenack), *Cometodinium habibi* Montail, *Systematophora areolata* Klement, *Prolixosphaeridium parvispinum* (Deflandre), *Prolixosphaeridium* spp., *Achomosphaera* sp., *Spiniferites* ex gr. *ramosus* (Ehrenberg); prasinophytes *Pterospermella*.

As a whole, the dinocyst assemblage in Berrasian sediments of central Crimea is characterized by an impoverished composition. Nevertheless, it is evident that by its taxonomic composition this assemblage is close to that from the Phoberocysta neocomica Beds.

## DEPOSITIONAL ENVIRONMENTS

The depositional environments of Berriasian sediments were relatively diverse, although as a whole they

**Plate IV.** Dinocysts from Berriasian sediments of central Crimea.

All the specimens originate from Berriasian section 2940 near the Balki settlement in central Crimea.

(Figs. 1–5, 8, 10–14, 17–23) occitanica Zone, tauricum Subzone, Member 20, Sample 149/13220; (figs. 6, 7, 9) occitanica Zone, tauricum Subzone, Member 21, Sample 147/13220; (figs. 15, 16) bossieri Zone, Symphythiris arguinensis Beds, Member 25, Sample 148/13220.

(1a, 1b) *Phoberocysta neocomica* (Gocht); (2) *Achomosphaera* sp.; (3) *Tanyosphaeridium isocalamum* (Defl. et Cook.); (4, 5) *Hystrichsphaerina*? *orbifera* (Klement); (6) *Oligosphaeridium patulum* Riding et Thomas; (7) *Epiplosphaera gochti* (Fens.); (8) *Cleistosphaeridium varispinosum* (Sarjent); (9) *Epiplosphaera ?areolata* (Klement); (10) *Kleithriasphaeridium eoinodes* (Eisen); (11) *Circulodinium distinctum* (Defl. et Cook.); (12) *Circulodinium brevispinosum* (Pocock); (13) *Dichadogonyaulax culmula* (Norris); (14) *Scrinodinium campanula* Gocht; (15, 16) *Systematophora* sp.; (17) *Apteodinium* sp.; (18) *Ctenidodinium* sp.; (19) *Dichadogonyaulax*? *pannea* (Norris); (20) *Nannoceratopsis deflandrei* Evitt subsp. *deflandrei*; (21) *Tanyosphaeridium* sp.; (22) *Micrhystridium* sp.; (23) *Pterospermella* sp.

Plate IV

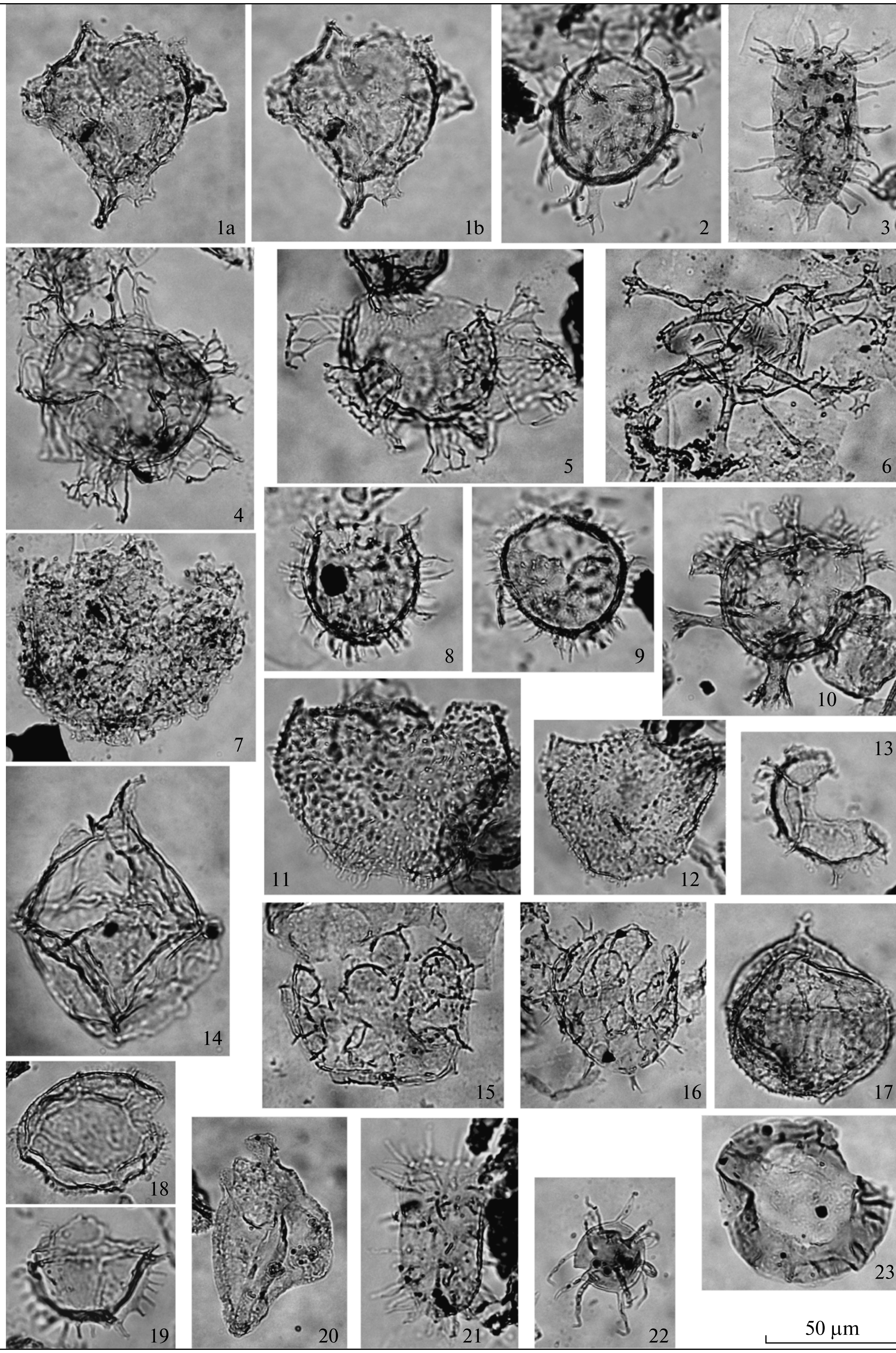

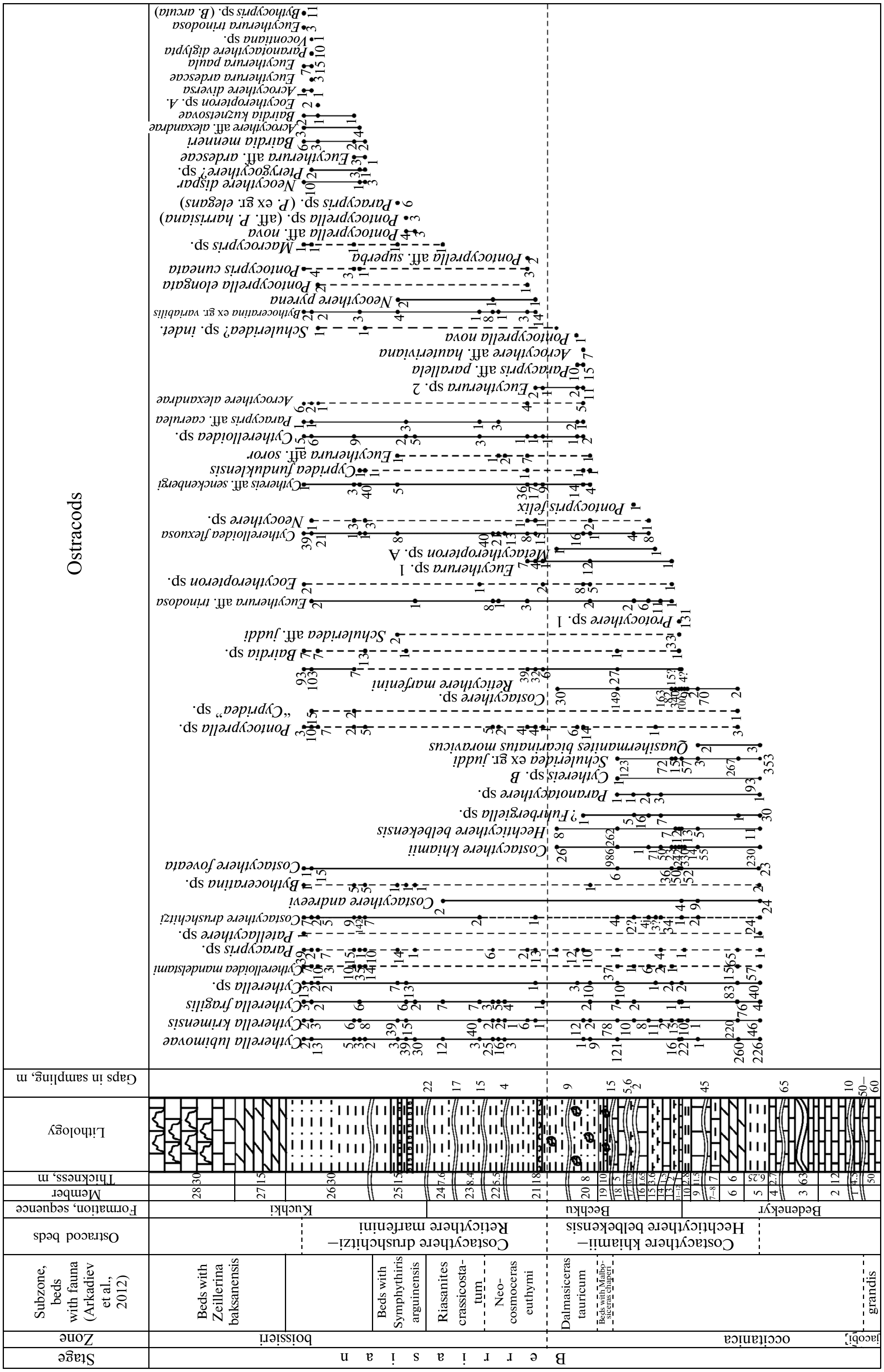


**Fig. 6.** Stratigraphic distribution of main ostracod species in Berriasian sections of central Crimea. For legend, see Fig. 4.

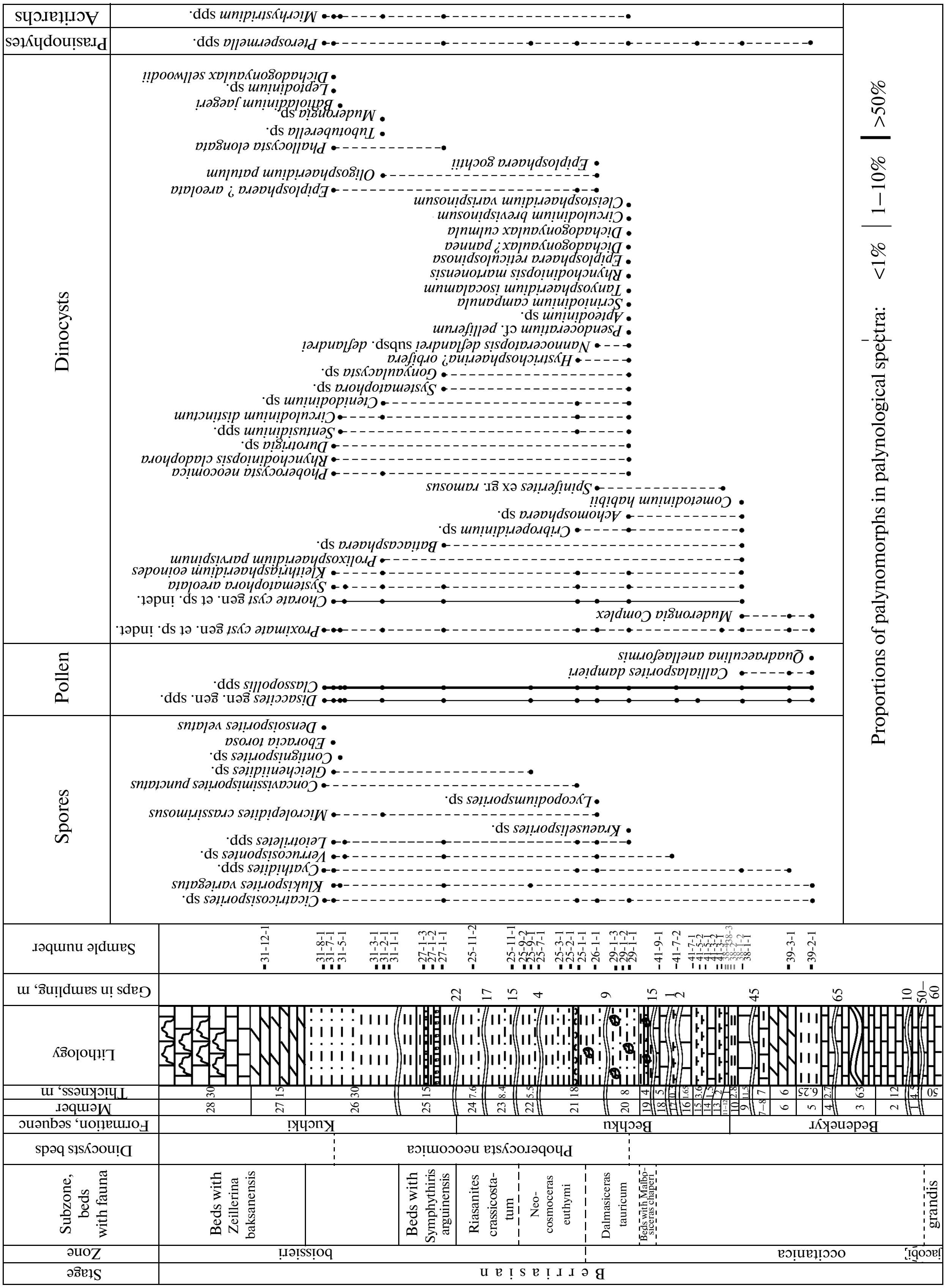


**Fig. 7.** Stratigraphic distribution of palynomorphs in Berriasian sections of central Crimea. For legend, see Fig. 4.

were always associated with development of the carbonate platform.

The lower part of the section (Members 1–18) demonstrates a relatively uniform composition of calcareous sediments in both the lateral and the vertical direction. The presence of clay and marlstone intercalations and the absence of features indicating extremely shallow areas, landslides, and accumulation of detrital sediments imply the formation of this part of the section in settings of an almost flat homoclinal ramp.

The examined limestone varieties belong to two ramp microfacies (RMF; Flügel, 2010):

(1) RMF 3 (Members 1–4, 18) is represented by wacke- and packstones with skeletal detritus bioturbated by crustaceans (*Thalassinoides*, Plate V, fig. 1). The presence of micrite, skeletal detritus, and ooids indicates calm to moderate hydrodynamics. This microfacies is characteristic of the middle and/or outer ramp.

(2) RMF 9 (Members 8, 9, 14, 16) comprises pack-, wacke-, and floatstones with bioclasts and intraclasts of the ramp, rare thalassinoid burrows, and lenses of shelly floatstones (SMF 8 after Flügel, 2010). This microfacies characterizes the middle and/or outer ramp and calm to moderate hydrodynamics. Skeletal detritus in both microfacies represents typical material redeposited from inner parts of the ramp.

The rare sandstone intercalations (Members 11, 12, Plate V, figs. 5, 6) with well-developed trough to horizontal bedding locally disturbed by crustacean *Ophiomorpha* burrows (Plate V, fig. 5) were probably deposited in tidal channels (Baraboshkin, 2011). The effect of high-energy currents is evident from the presence of oyster accumulations with separated valves (Plate V, fig. 3).

Clays and marlstones (Members 5, 6, 10, 13, 15, 17, partly 18) were deposited in inner areas of the basin and/or in depressions; in either case, they indicate deeper sedimentation settings as compared with depositional environments of limestones. Corals of the genus *Montlivaltia* occur frequently in pelitic rocks (Wright and Burgess, 2005); therefore, their co-occurrence with belemnites and ammonites in Member 15 implies their autocthonous nature. At the same time, it is conceivable that accumulation of some clay members as well as the entire terrigenous part of the section was stimulated by climate humidization, which explains the presence of carbonaceous detritus, sand admixture, and coquinas.

Thus, the lower calcareous part of the section (Members 1–4) was accumulated in environments of the middle and/or outer ramp, while its overlying part dominated by clays and marlstones was deposited in deeper settings of inner areas of the basin or under climate humidization. Taking into consideration the insignificant lateral variability of sediments in outer parts of the ramp (Tucker and Wright, 1990; Flügel, 2010) and low probability of the replacement by carbonate facies, the vertical replacement of limestone by clays resulted from transgressive processes or climate humidizatiuon. The basin deepening is consistent with the transgressive part of the megacycle in other regions corresponding to the jacobi and occitanica phases (Ogg and Hinnov, 2012).

The overlying part of the section (Members 19–24) is largely represented by the terrigenous succession. Its basal layers are composed of bioturbated glauconite–quartz carbonate sandstones grading up the section into clays with abundant small pyritized shells of ammonites and other faunal remains. This trend most likely reflects the basin deepening stage.

The appearance of the sponge horizon (Member 25) reflects the change in the basin dynamics. The absence of features indicating the dynamic influence of water and the presence of a significant mud component in sediments indicate that the sponge horizon was formed at depths exceeding 50 m. The growth of *Spongia* bioherms proceeds usually under the influence of high-energy bottom currents, which transport food particles and nutrients. Such bioherms grow near the slope bends; it is conceivable that, this area corresponded to the middle–lower ramp transition or was slightly deeper.

The overlying section (Members 26–28) demonstrates a well-expressed shoaling trend, which is also consistent with the transgressive–regressive megacycle of the boissieri phase (Ogg and Hinnov, 2012). The regressive features are already evident in the upper part of Member 25 (Plate V, fig. 7), which was formed in relatively shallow environments of the warm basin. However, the substantial share of silty–sandy terrigenous admixture prevented accumulation of pure carbonate sediments in this zone. At the same time, the presence of *Ophiomorpha* burrows implies an unconsolidated mobile substrate. The higher carbonate content in Members 26–27 and the presence of abundant remains of diverse normal-marine organisms, including oysters, brachiopods, and echinoderms, indicate open basin (ramp?) settings with the dominant role of tidal currents. The section is crowned by Member 28, represented by coral–rudist–algae limestones

**Plate V.** Fragments of the section structure and some ichnofossils in Berriasian sediment.

(1) *Thalassinoides suevicus* (Rieth) burrow, Member 3; (2) *Gyrolithes* sp. burrow, presumably Members 10–12; (3) accumulation of oyster *Pycnodonte weberae* Yanin shells, Member 12; (4) limestones entirely bioturbated by *Thalassinoides* burrows, Member 2; (5) horizontally bedded sandstones with *Ophiomorpha* sp. (arrow), Member 12; (6) trough cross bedding in sandstones, some layers are enriched with bioclasts, Member 12; (7) outcrops of Member 25 near the Pasechnoe settlement; (8) outcrops of Member 28 (biohermal limestones) in the quarry of the Pasechnoe settlement, the top of the quarry wall corresponds to the presumable Berriasian–Valanginian boundary. (Figs. 1–6) Balki settlement area, photo by V.K. Piskunov, 2012; (figs. 7, 8) photo by E.Yu. Baraboshkin, 2002.

Plate V

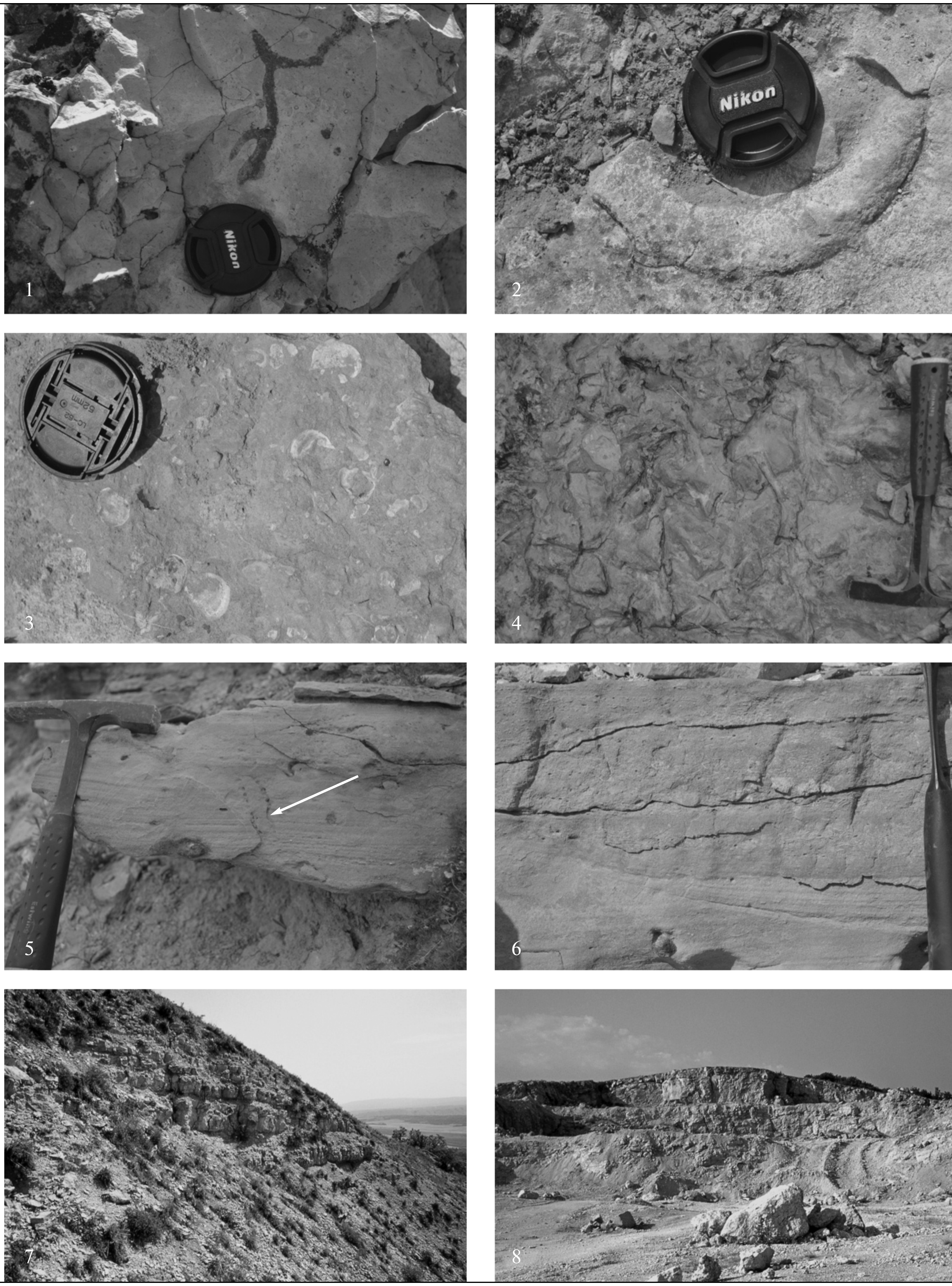

(Plate V, fig. 8), which were deposited on the coastal shoal raised intermittently above the sea level.

The Berriassian sedimentation stage terminates with desiccation of the carbonate platform, which was accompanied by karst processes and reorganization of the sedimentary system: in the Valanginian, terrigenous sedimentation became prevalent.

Most identified ostracod taxa are characteristic of basins with normal salinity. Single representatives of their genera able to resist salinity variations or dwell in brackish-water to fresh-water environments do not effect on in their general distribution (Morkhoven, 1963; *Prakticheskoe*..., 1999 ). The results of the paleoecological analysis of ostracod assemblages are also consistent with presumable basin deepening (Members 5–18) and shoaling (Member 26) and confirm the conclusion on deposition of the sponge horizon (Member 25) at depths exceeding 50 m.

The palynological data (Fig. 7), including abundant *Classopollis* spp. pollen (up to 90% in spectra) produced by Cheirolepidaceae plants and dominant role of chorate dinocysts with long processes, imply warm (tropical) environments.

## MAGNETOSTRATIGRAPHY

### *Petromagnetic and Magnetic–Mineralogical Investigations*

The petromagnetic and magnetic–mineralogical investigations included the study of magnetic susceptibility ($K$) and its anisotropy (AMS), measurement of remanent magnetization ($\mathbf{J_n}$), experimental magnetic saturation with subsequent determinations of remanent magnetization of saturation ($\mathbf{J_{rs}}$) and remanent coercive force ($H_{cr}$), and differential thermomagnetic analysis (DTMA). $K$ was measured on MFK1-FB equipment (kappabridge), $\mathbf{J_n}$ was measured on a JR-6 spin magnetometer, and a TAF-2 thermoanalyzer of fractions ("magnetic weights") was used for DTMA. The AMS analysis was conducted using the Anisoft 4.2 program.

The composite section is well differentiated with respect to its petromagnetic properties (Fig. 8).

The lower (carbonate) part of the section (Members 1–9) is slightly magnetized ($K = 0.2–8 \times 10^{-5}$ SI units, $\mathbf{J_n} = 0.002–0.2 \times 10^{-3}$ A/m).

The overlying terrigenous sediments (Members 10–26) are characterized by higher $K$ values increasing up the section to $25–33 \times 10^{-5}$ SI units in Members 20–22 and then gradually decreasing to $11–15 \times 10^{-5}$ SI units in Member 26. The similar trend in the distribution of $\mathbf{J_n}$ values is complicated by the presence of several intervals with abnormally high values, which results in the increase in the Konigsberger ratio ($Q$ factor) to several units, while its background values never exceed fractions of unity. The upper carbonate members (27 and 28) are slightly magnetic ($K = 1–3 \times 10^{-5}$ SI units, $\mathbf{J_n} = 0.01–0.1 \times 10^{-3}$ A/m).

The $K/\mathbf{J_{rs}}$ parameter proportional to the average size of ferromagnetic particles is lowest in clays of the Bechku Formation (Members 19–24) and highest in limestones of Members 3 and 4 and terrigenous–carbonate varieties of Members 26 and 27.

$H_{cr}$ value is highly variable ($20–325 \times 10^3$ A/m), being highest in some carbonate varieties of Members 1–4, 9, 27, and 28. Many samples are magnetically soft (saturation is achieved in fields of $\sim 100 \times 10^3$ A/m) (Fig. 9a), which is determined by the presence of magnetite or close minerals. The magnetically hard samples do not achieve saturation in fields up to $600 \times 10^3$ A/m (Fig. 9b), which is explained by the presence of hematite or strongly dehydrated Fe hydroxides. On saturation curves obtained for limestones from the lower part of the section (Members 1–3), both phases (magnetically soft and hard) are well recognizable (Fig. 9c).

The presence of magnetite is also evident on DTMA curves. Unfortunately, the peak near 550–578°C corresponding to the Curie point of $Fe_3O_4$ or close minerals is masked on all of them by thermomagnetic effects related likely to pyrite. The presence of the latter is evident from the magnetization increment above 400°C owing to transformation of $FeS_2$ into $Fe_3O_4$ (Figs. 9d, 9e). The magnetically hard phase (hematite, martite, or dehydrated Fe hydroxides) is reflected in the poorly expressed peak on DTMA curves in the area of 650°C (Fig. 9e).

The ASM patterns are different in carbonate and terrigenous varieties. Limestones exhibit chaotic magnetic patterns (Fig. 9f), while in clays and sandstones projections of short axes of magnetic ellipsoids are regularly grouped in the center of the stereographic projection and projections of long axes strive to the equator and are marked by slight but distinct anisotropy along the sublatitudinally oriented line that corresponds with the strike of beds (Fig. 9g). In order to exclude suspicions that chaotic AMS patterns (Fig. 9f) are determined by the instrumental error in measurements of slightly magnetic limestones (mostly $K < 3 \times 10^{-5}$ SI units), we have analyzed two selections of samples with the measurement errors of <5% and >5%, respectively. The testing revealed that the magnetic patterns in both selections are the same.

The anisotropy of magnetic susceptibility in limestones is most likely determined by the irregular distribution of ferromagnetic minerals due to their concentration in bioturbations, which are characteristic of carbonate rocks in the examined section. The enrichment of ichnofossils with ferromagnetic minerals is explained by the concentration of biogenic magnetite in many crustacean organisms (Biskirk and O'Brian, 1989); in addition, some burrows become populated by magnetite-producing bacteria (Stolz et al., 1986). Bioturbation of sediments provides no obstacle for paleomagnetic investigations since ferromagnetic particles remain oriented in accordance with the field in semiliquid sediments acquiring the post-depositional detrital remanent magnetization $\mathbf{J_n}$.

The anisotropy of long axes of magnetic ellipsoids in the terrigenous part of the section indicates com-

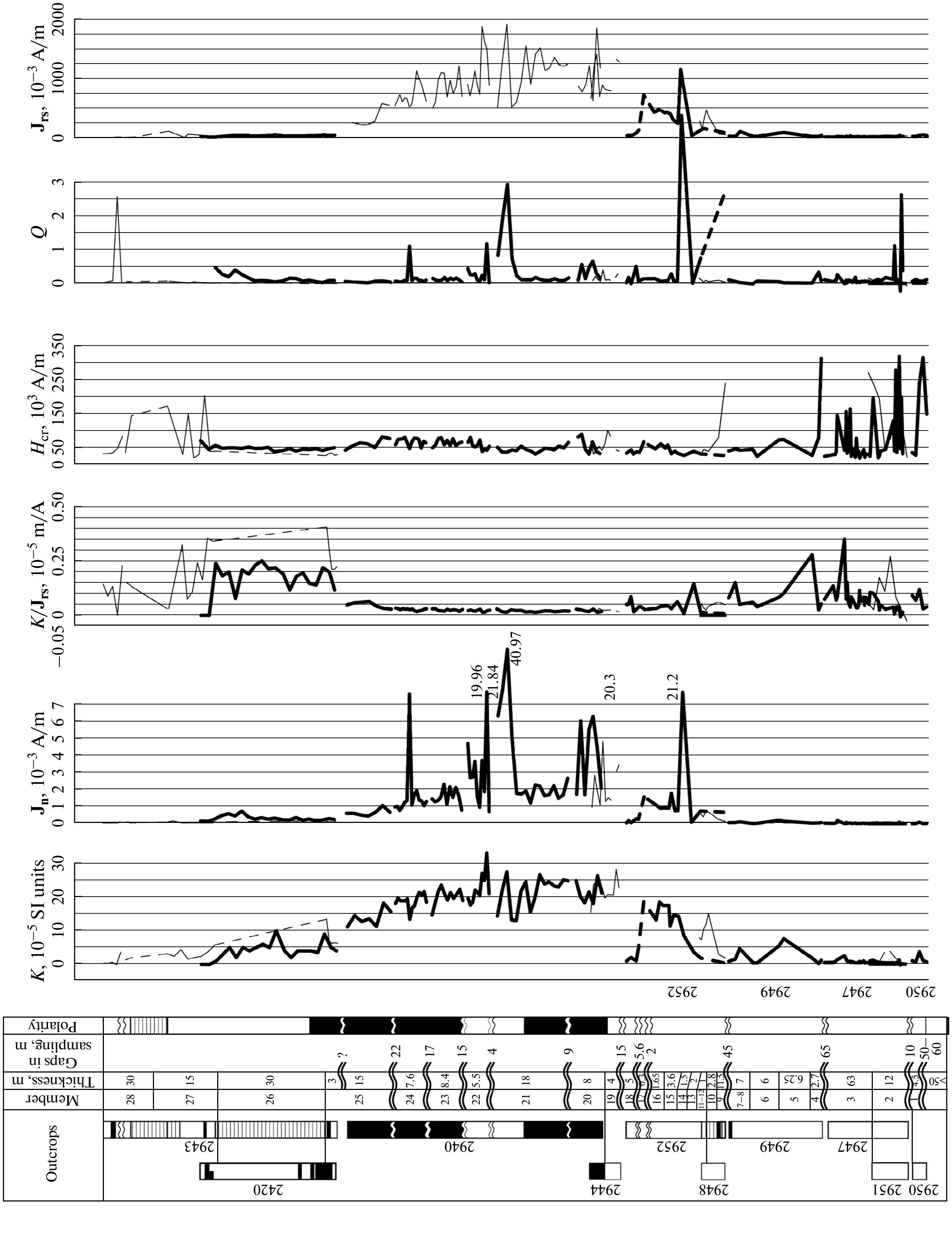

**Fig. 8.** Composite magnetostratigraphic Berriasian section of central Crimea: paleomagnetic and petromagnetic characteristics. For legend, see Fig. 4.

pression of rocks in the submeridional direction, which is consistent with widely shared views on geodynamics of the Crimean Peninsula at the neotectonic stage (Nikishin et al., 1997). In contrast to hard limestones, clays and clayey sands changed their magnetic structure in response to collisional compressions. At the same time, judging from the vague anisotropy of long axes, deformations which they experienced could not have resulted in significant distortion of $\mathbf{J_n}$ vectors able to affect polarity determination.

An atypical AMS distribution is documented in outcrop 2952 represented by alternating carbonate and terrigenous rocks. As in the remaining section, limestones in this outcrop are characterized by chaotic magnetic patterns. At the same time, projections of short axes in clays (Members 13, 15, 17) are displaced from the center of the stereographic projection and are arranged along a large circle in the SE–NW direction, while long axes are distributed transversely in the SW–NE direction (Fig. 9h). Such magnetic patterns indicate that these rocks were subjected to extremely intense deformations due to local compression along the SE–NW axis (Lanza and Meloni, 2006), which was probably accompanied by the formation of the upthrown (thrust) structure. This conclusion is indirectly confirmed by development of cleavage in limestones (Member 18) and poor quality of the paleomagnetic record in this outcrop. In such a situation, the data on this interval of the section, including documented succession of layers, should be taken with precaution. It is conceivable that limestones with intense cleavage represent an exotic block (klippe) of older strata, which is consistent with the paleontological data: the foraminiferal assemblage from Member 18 differs from that in underlying terrigenous rocks, being identical to the assemblage in older limestones.

Similar AMS patterns are observed in clays, siltstones (upper part of Member 25 and Member 26), and marlstones (Member 27) cropping out in the Mezhgor'e and Pasechnoe areas (outcrops 2943, 2420): projections of short axes of magnetic ellipsoids demonstrate as in outcrop 2952 a tendency for the shift along the large circle, although they are less remote from the center of stereographic projection (Fig. 9i). This indicates that unconsolidated plastic sediments are deformed by compression in the SE–NW direction (as in outcrop 2952, but to a lower degree).

Thus, the AMS investigations make it possible to obtain nontrivial information on intensity of tectonic movements, which affected rocks in the region under consideration, and, in fact, to specify the structure of the Berriasian section in central Crimea. At the same time, outcrops 2952, 2943, and 2420 (Members 13–18, 26–28) appeared to be unfavorable objects for paleomagnetic investigations. As a whole, variations in petromagnetic parameters through the composite section promote individualization of its particular intervals and recognition of sedimentation cyclicity (Fig. 8), which is of undoubted interest for substantiation of stratigraphic units and paleogeographic reconstructions.

### *Paleomagnetic Investigations*

The paleomagnetic investigations were aimed at obtaining magnetic polarity characteristics of the section. Each of 181 oriented samples taken from different stratigraphic levels (Figs. 3, 4) was cut into three or four cubes with edges of 20 mm. The laboratory investigation of the samples included $\mathbf{J_n}$ measurements on the JR-6 spin magnetometer after a series of successive magnetic demagnetization sessions by an alternating field mostly up to 45–60 mT with a step of 5 mT (H demagnetization) on LDA-3 AF equipment and temperature ranging from 100°C to 500–550°C with a step of 50°C (T° demagnetization) in an Aparin furnace. The samples were subjected to the impact of high fields and temperatures until their magnetization became comparable with the instrumental measurement accuracy. For the control over the possible laboratory magnetization of samples, two cubes from the same sample with mutually opposite orientation along two $\mathbf{J_n}$ constituents were placed into the furnace. For the control over the quality of results, some samples were measured on the cryogenic magnetometer (2G Enterprises) in the Paleomagnetic Laboratory (Institute of Petroleum Geology and Geophysics, Siberian Branch, Russian Academy of Sciences, Novosibirsk). The data were processed using the Remasoft 3.0 program. The natural remanent magnetization ($\mathbf{J_n}$) retained after the impact of strong fields and high temperatures was accepted as the stable component of magnetization (SCM) (Figs. 10a, 10b).

Carbonate rocks of the basal part of the section appeared to be most favorable for paleomagnetic investigations. In samples from these rocks, the stable components of magnetization projected onto the upper hemisphere are usually defined with the appropriate accuracy (maximum deviation angles up to 15°) after both demagnetization procedures (Fig. 10a). The results of thermal demagnetization of samples from Members 1–3 yield better paleomagnetic statistics as compared with that for backup samples, where $\mathbf{J_n}$ was

**Fig. 9.** Results of the magnetic–mineralogical analysis. (a–c) Curves of magnetic saturations; (d, e) DTMA curves (integral curves and first derivatives according to thermomagnetic analysis curves); (f–j) distributions of directions for axes of anisotropy of magnetic susceptibility (in the stratigraphic coordinate system) for limestones (f) and terrigenous rocks (g) from outcrops 2952 (h) and 2943 (i). DTMA was conducted simultaneously for several lithologically and magnetically similar samples. (1, 2) Long (*K*1) and short (*K*3) axes of ellipsoid of anisotropy of magnetic susceptibility, respectively.

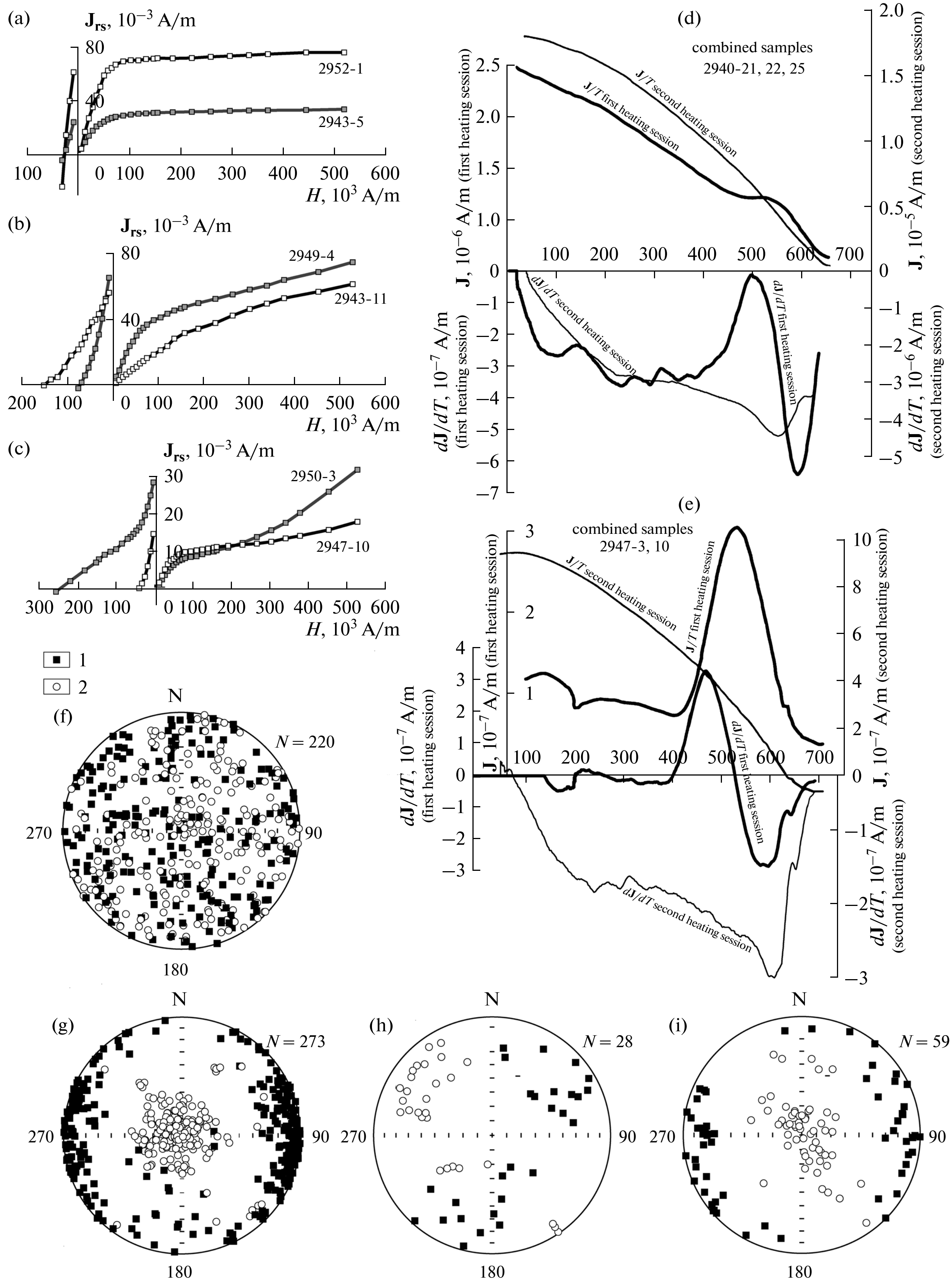
(a)
Jrs, 10−3 A/m
2952-1
2943-5
H, 10³ A/m
(b)
Jrs, 10−3 A/m
2949-4
2943-11
H, 10³ A/m
(c)
Jrs, 10−3 A/m
2950-3
2947-10
H, 10³ A/m
(d)
combined samples
2940-21, 22, 25
J/T second heating session
J/T first heating session
dJ/dT second heating session
dJ/dT first heating session
J, 10−6 A/m (first heating session)
J, 10−5 A/m (second heating session)
dJ/dT, 10−7 A/m (first heating session)
dJ/dT, 10−6 A/m (second heating session)
(e)
combined samples
2947-3, 10
J/T second heating session
J/T first heating session
dJ/dT first heating session
dJ/dT second heating session
J, 10−7 A/m (first heating session)
J, 10−7 A/m (second heating session)
dJ/dT, 10−7 A/m (first heating session)
dJ/dT, 10−7 A/m (second heating session)
1
2
(f)
N = 220
(g)
N = 273
(h)
N = 28
(i)
N = 59
N
90
180
270

destroyed by the alternating field (table). The relatively high precision parameter and steeper (than after H demagnetization) paleomagnetic inclination are determined by the fact that magnetization related to hard ferromagnetic minerals is destroyed by temperature more effectively. This is evident from the correlation between the precision parameter and $H_{cr}$ values in results of demagnetization by the alternating field: in the magnetically softest samples, precision parameters are the highest and paleomagnetic directions correspond to the vector derived from thermal demagnetization sessions, the precision parameter decreases with addition of magnetically harder samples to the selection, and the average paleomagnetic inclination becomes gentler (table).

In terrigenous varieties, the reliability of paleomagnetic measurements is worse than in limestone, although the *K* and $\mathbf{J_n}$ values in them are substantially higher. No stable component was defined in approximately one-third of terrigenous samples. The remaining samples may be divided into two groups. In samples of the first group, $\mathbf{J_n}$ projections either were initially located on the northern sector of the lower hemisphere or left it after the session of demagnetization by weak temperature and alternating field. Such behavior of paleomagnetic vectors during demagnetization was interpreted as the presence of the $\mathbf{J_n}$ component corresponding to the reversed polarity (R). In some sample, SCM is anomalous: for example, southerly declination combined with positive inclinations in Sample 2940-30 (Fig. 10c). In samples of the second group, projections of paleomagnetic vectors remained in the northern sector of the lower hemisphere up to the last session of demagnetization (Fig. 10b). These directions are interpreted as corresponding to normal polarity of the magnetic field (N).

We believe that the significant scatter of R vectors (Figs. 10e, 10f) is determined by the different degree of **SCM** "contamination" with the stabilized secondary component related to products of oxidation of magnetic grains and by impossibility to separate the components during demagnetization. This effect leaves the paleomagnetic statistics on normally magnetized samples practically unchanged (Fig. 10g, table) since SCMs corresponding to normal polarity are close to the direction of rock magnetization reversal by the recent field, although statistically being different (table).

It is of importance that the results of the sample magnetization reversal by the alternating field and temperature demonstrate principal similarity (Figs. 10c, 10d). This increases substantially the reliability of paleomagnetic measurements as compared with the results based only on one of the demagnetization procedures. Nevertheless, the anomalous reversed polarity is shown as the half-shaded paleomagnetic column in Figs. 3 and 4. The rejected and unreliable polarity determinations are scattered more or less regularly through the section; therefore, the absence of information hardly affects its paleomagnetic structure.

Small gaps in polarity determinations and single intervals with its opposite sign were ignored during compilation of the composite paleomagnetic column (Figs. 2, 11). Owing to the biostratigraphic control, identification of the paleomagnetic column with successive magnetic chrons was successful (at least for Members 1–23) despite large unexposed intervals and doubts in the reliability of results obtained for some intervals of outcrops 2952, 2943, and 2420. The long R magnetic zone corresponding to the largest part of the occitanica Zone (and, probably, uppermost jacobi Zone) and N magnetic zone in the uppermost part of the occitanica Zone represent undounbted analogs of Chron M17 (M17r and M17n, respectively). The Dalmasiceras tauricum Subzone is an analog of the Dalmasiceras dalmasi Subzone of the Mediterranean standard and consequently Chron M17n cannot correspond to large gaps in sampling between Members 3 and 4 or 8 and 9 (Figs. 2, 11), which are located considerably below the first finds of *Dalmasiceras* representatives. The overlying R magnetic zone corresponds to Chron M16r established previously in the Feodosiya area (Arkadiev et al., 2010) (Fig. 11). The examined section includes also analogs of Chrons M16n and M15r (it is conceivable that M15n and M14r are included as well), although their position cannot be determined because of large gaps in sampling (Fig. 11).

The obtained data make it possible to carry out magnetostratigraphic correlation of the Berriasian section of central Crimea and the Berriasian stratotype

**Fig. 10.** Results of the component analysis.

(a, b) (From left to right) stereographic images of changes in $\mathbf{J_n}$ vectors during demagnetization sessions, Zijderveld diagrams, demagnetization plots; (c, d) comparison of results of demagnetization by the alternating field (*h*) and temperature (*t*); (e–g) stereographic projections of SCM corresponding to R polarity in Members 1–3 (limestones) according to results of T° and H demagnetization (e), R polarity in Members 5–25 (terrigenous rocks) according to results of T° and H demagnetization (f), R polarity in Members 1–3 (limestones) according to results of H demagnetization of magnetically softest samples ($H_{cr}$ = 19.6–26.8 × $10^3$ A/m) and T° demagnetization, and N polarity in Members 5–25 (terrigenous rocks) according to results of T° and H demagnetization (g). All the Zijderveld diagrams and $\mathbf{J_n}$ stereographic projections are presented in the stratigraphic coordinate system. (1, 2) $\mathbf{J_n}$ projections in stereograms on the lower (1) and upper (2) hemispheres; (3, 4) projections of average SCM directions for all R and N populations of vectors, respectively; (5) projections of directions of rock magnetization reversal by the recent geomagnetic field ("crosses" of magnetization reversal).

Paleomagnetic statistics for the stereogram (c) and interpretation of statistical parameters are presented in the table.

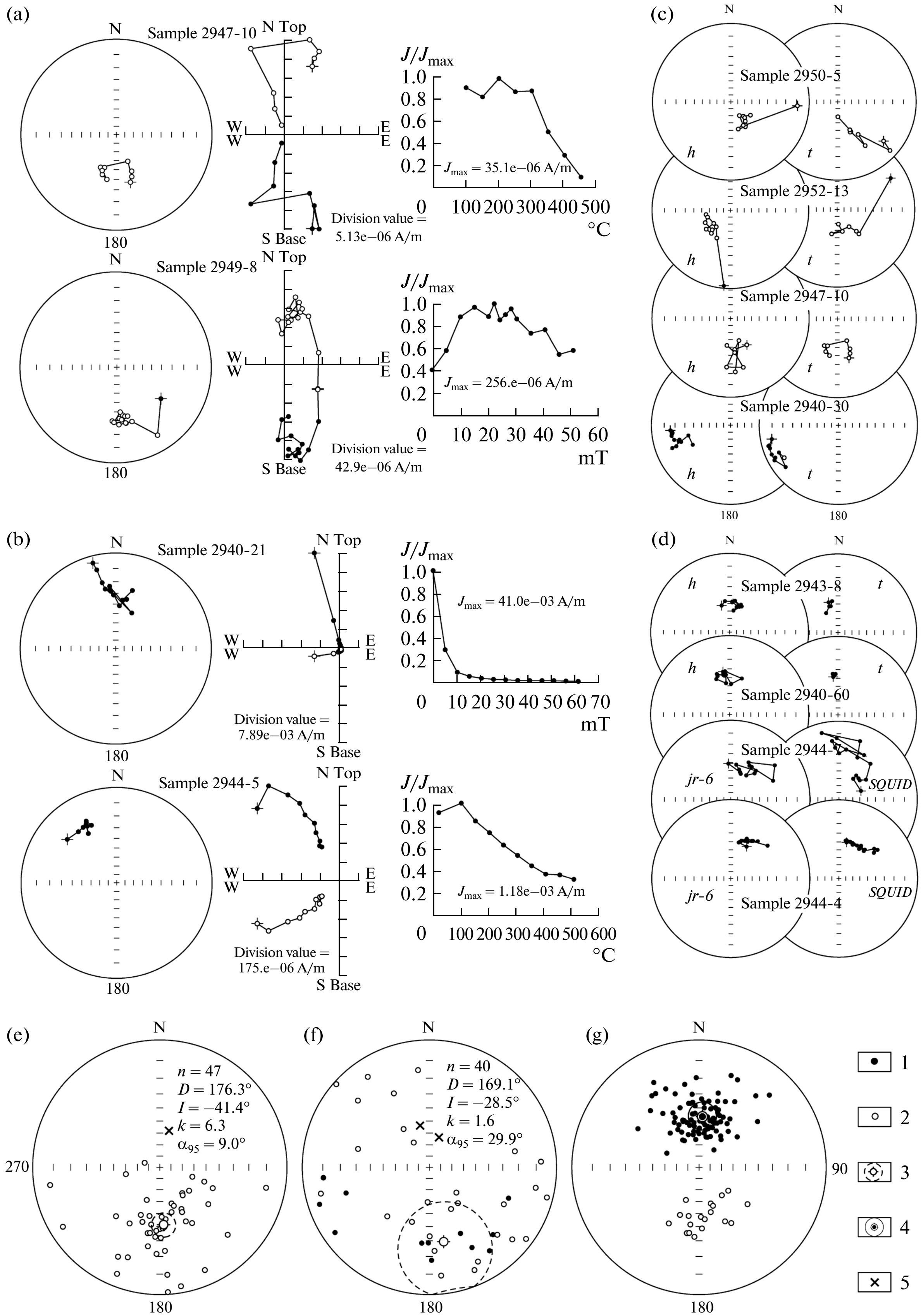
(a)
N
180
Sample 2947-10
N Top
W
E
S Base
Division value = 5.13e–06 A/m
$J/J_{max}$
$J_{max}$ = 35.1e–06 A/m
°C
Sample 2949-8
Division value = 42.9e–06 A/m
$J_{max}$ = 256.e–06 A/m
mT
(c)
Sample 2950-5
Sample 2952-13
Sample 2947-10
Sample 2940-30
h
t
(b)
Sample 2940-21
Division value = 7.89e–03 A/m
$J_{max}$ = 41.0e–03 A/m
Sample 2944-5
Division value = 175.e–06 A/m
$J_{max}$ = 1.18e–03 A/m
(d)
Sample 2943-8
Sample 2940-60
Sample 2944-7
Sample 2944-4
jr-6
SQUID
(e)
$n = 47$
$D = 176.3°$
$I = –41.4°$
$k = 6.3$
$\alpha_{95} = 9.0°$
270
(f)
$n = 40$
$D = 169.1°$
$I = –28.5°$
$k = 1.6$
$\alpha_{95} = 29.9°$
(g)
90
1
2
3
4
5

in France (Galburn, 1985) (Fig. 11) and combined with the available data on eastern Crimea (Arkadiev et al., 2010; Bagaeva et al., 2011; Guzhikov et al., 2012) allow the statement that analogs of all the Berriasian magnetic chrons are present in Crimea.

The ancient nature of the stable component of magnetization (SCM) is substantiated by the following arguments.

(1) The direction of geomagnetic polarity is independent of both the lithological composition of rocks and variations in their petromagnetic properties (Figs. 2, 8). This does not prove the hypothesis of the old magnetization nature, but is consistent with the latter since the geomagnetic reversal is a global phenomenon; therefore the probability of interrelations between magnetic polarity and lithological–magnetic properties determined by local and regional factors is negligible.

(2) The data on magnetic patterns of limestones (Fig. 9f) imply the confinement of the magnetically soft fraction to bioturbations, indicating the biogenic nature of magnetite particles, which could not have been formed later than the diagenetic stage.

The entire section exhibits features characteristic of detrital magnetization and, in contrast, atypical of chemical magnetization: low Q factor values (fractions of unity) except for narrow intervals (to 1–5) sporadically scattered through the section (Fig. 8) and low paleomagnetic interstratal precision parameters (up to 30) (table).

The substantiation of the hypothesis of sediment magnetization prior to diagenesis cessation is identical to the proof that $\mathbf{J_n}$ reflects the direction of the geomagnetic field in the Berriasian.

(3) The most reliable paleomagnetic result obtained for limestones (table) is statistically identical to the average paleomagnetic direction available for the Late Jurassic in western Crimea (Pecherskii and Safonov, 1993) (it should be noted that, according to D.M. Pecherskii, “western Crimea” includes the Ai-Petri Yala, Karabi-Yaila, Demerdzhi, Chatyr Dag, and Cape Fiolent areas).

(4) The paleomagnetic reversal (inversion) test is positive (table), which represents a very solid argument in favor of the primary nature of magnetization.

(5) The paleomagnetic zonality of the composite section is well consistent with traditional views on the regime of the Berriasian geomagnetic field (Ogg and Hinnov, 2012) (Fig. 11).

The index of paleomagnetic confidence for the obtained data is formally equal to 6 (of 7 possible) according to the classification in (Van der Voo, 1997) and 7 (of possible 8) according to A.N. Khramov in (*Dopolneniya*..., 2000). Thus, magnetic polarity determinations for the largest part of the Berriasian section (Members 1–23) deserve credence despite the generally low paleomagnetic quality of examined rocks.

## CONCLUSIONS

(1) The contact between the carbonate Bedenekyr and terrigenous Bechku formations is described for the first time for central Crimea with the age of the upper part of the former unit attributed to the Berriasian occitanica Zone being specified.

(2) On the basis of the combined paleontological and magnetostratigraphic data, the Malbosiceras chaperi Beds are attributed to the occitanica Zone.

(3) Six successive foraminiferal assemblages are defined through the Berriasian section (from the base upward): (1) *Everticyclammina virguliana–Retrocyclammina recta–Bramkampella arabica*; (2) *Lenticulina muensteri*; (3) *Quadratina tunassica*; (4) *Triplasia emslandensis acuta*; (5) *Lenticulina andromede*; (6) *Conorboides hofkeri*.

(4) The ostracod assemblages provide basis for defining the following biostratigraphic units in the Beriassian section (from the base upward): Costacythere khiamii–Hechticythere belbekensis Beds correlated partly with the ammonite occitanica Zone and the Costacythere drushchitzi–Reticythere marfenini Beds correlated partly with the ammonite boissieri Zone.

(5) The dinocysts assemblage allows the Phoberocysta neocomica Beds correlated partly with the ammonite occitanica and boissieri zones to be defined.

(6) A series of isolated outcrops (Novoklenovo, Balki, and Mezhgor’e settlements) are united into a composite section, which represents now the most complete Berriasian succession for central Crimea. Owing to magnetostratigraphic data obtained for this composite section, the presence of all the Berriasian magnetic chrons in central and eastern Crimea is substantiated for the first time.

(7) On the basis of paleomagnetic data, the Berriasian section of central Crimea is correlated with its stratotype in the Mediterranean region with the position of standard Berriasian zones being specified.

(8) The established anisotropy in magnetic susceptibility is used for reconstructing directions of deformations of terrigenous (clayey) rocks in response to tectonic movements.

## ACKNOWLEDGMENTS

We are grateful to S.V. Lobacheva (posthumously) for identifying brachiopods, V.A. Perminov (Center of Learning Youth (TSENTUM) Intellekt, Feodosiya, Russia) for his help in organizing field works, A.Yu. Kurazhkovskii (Borok Geophysical Observatory) for help in conducting magnetic–mineralogical investigations, and N.V. Platonova (assistant to the director of the Resource Center X-ray Diffraction Research Methods of St. Petersburg State University) for accomplishing the X-ray phase analysis of samples.

Statistical parameters of the distribution of the stable component of magnetization (**SCM**) directions

| ($n$) number of samples in the selection<br>($D_{av}$, $I_{av}$) average paleomagnetic declination and inclination, respectively<br>($k$) precision parameter<br>($\alpha_{95}$) radius of the vector confidence circle | | | Polarity | $n$ | $D_{av}$ (°) | $I_{av}$ (°) | $k$ | $\alpha_{95}$ (°) | **Results of the reversal test** (McFadden and McElhinny, 1990) | | | When an angle exceeds the error value (±), the vectors demonstrate significant difference; in the opposite situation, they are statistically coincident (Debiche and Watson, 1995) | |
|---|---|---|---|---|---|---|---|---|---|---|---|---|---|
| | | | | | | | | | $A$ (°) | $A_c$ (°) | Cl | Angle with **RF** (°) | Angle with **SCM** + 180 (°) |
| Members 1–3 (limestones) | H demagnetization<br>All samples $H_{cr} = 45.4 - 325.4 \times 10^3$ A/m | | R | 33 | 177.9 | –37.1 | 5.0 | 12.5 | | | | | |
| | Magnetically soft | $H_{cr} = 19.6–26.8 \times 10^3$ A/m | R | 5 | 177.5 | –45.7 | 30.7 | 14.0 | | | | | |
| | | $H_{cr} = 19.6–27.7 \times 10^3$ A/m | R | 7 | 182.6 | –39.5 | 11.3 | 18.7 | | | | | |
| | | $H_{cr} = 19.6–30.9 \times 10^3$ A/m | R | 9 | 182.9 | –38.2 | 10.6 | 16.6 | | | | | |
| | T° demagnetization | | R | 14 | 172.0 | –47.9 | 16.1 | 10.2 | | | | | |
| | Stable component of magnetization (**SCM**) calculated using H demagnetization data on magnetically softest samples ($H_{cr}$=19.6–26.8 × $10^3$ A/m) and T° demagnetization | | R | 19 | 173.5 | –47.4 | 19.0 | 7.9 | 5.6 | 8.8 | B | | |
| Members 5–28 (terrigenous rocks) | | | N | 91 | 1.7 | 46.8 | 14.7 | 4.0 | | | | 11.8 ± 4.4 | 4.5 ± 6.7 |
| **SCM** + 180° | | | | | 353.5 | 47.9 | | | ($A$) angle between vectors<br>($A_c$) critical angle<br>(Cl) classification | | | 12.5 ± 6.7 | |
| Magnetization reversal by the recent field (**RF**) | | | | 2 | 4.3 | 58.7 | | 10 | | | | | 12.6 ± 6.1 |
| Western Crimea ($J_3$) (Pecherskii and Safonov, 1993) | | | | 11 | 352 | 47 | 102.8 | 4.5 | | | | 13.7 ± 3.2 | 1.1 ± 6.8 |

The amplitude of the secular geomagmetic variation (10%, according to V.G. Bakhmutov, 2006; (1200) summer variation is characterized by the amplitude of 8%).

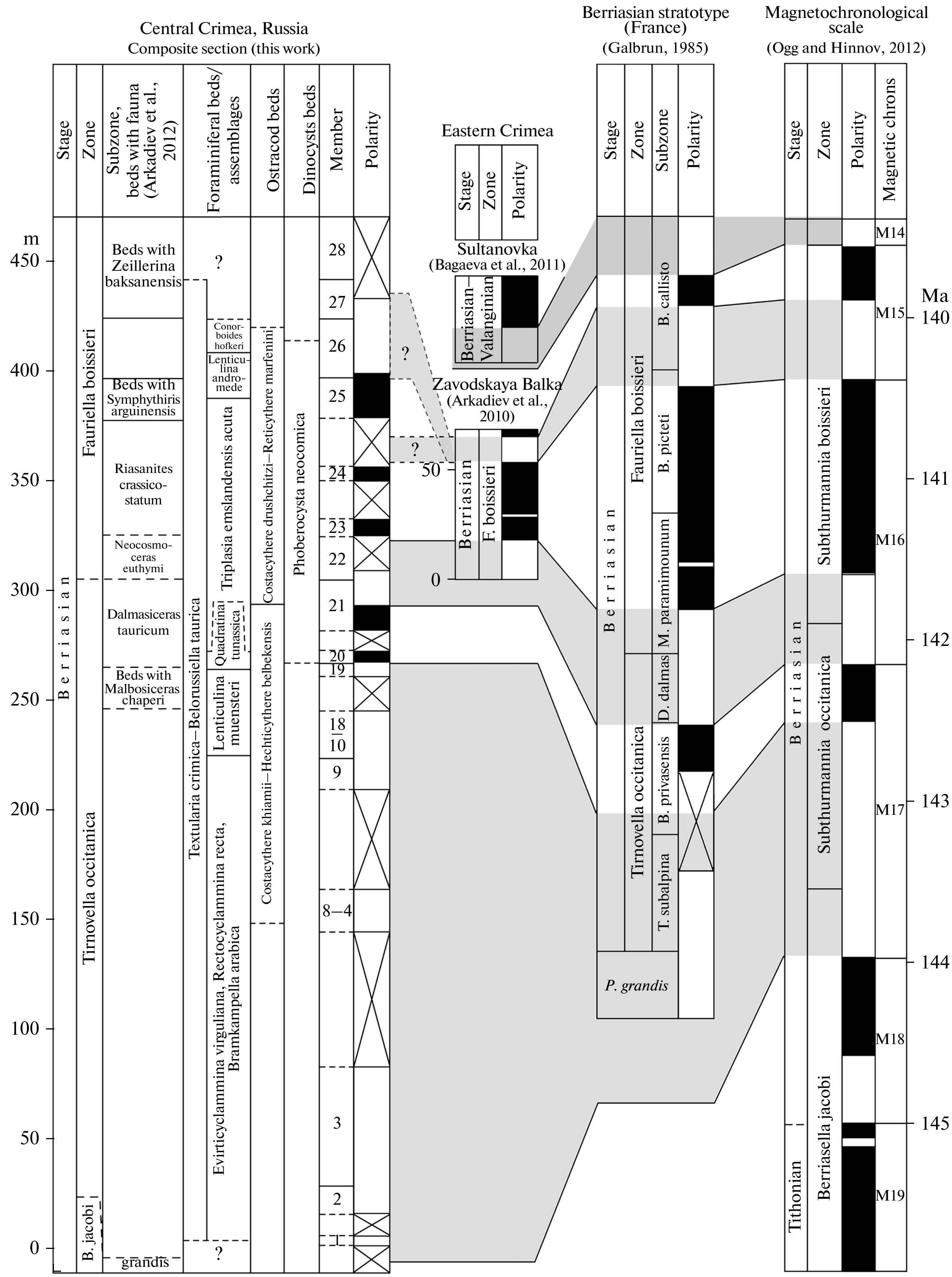
Central Crimea, Russia
Composite section (this work)
Stage
Zone
Subzone, beds with fauna (Arkadiev et al., 2012)
Foraminiferal beds/assemblages
Ostracod beds
Dinocysts beds
Member
Polarity
Eastern Crimea
Sultanovka
(Bagaeva et al., 2011)
Berriasian–Valanginian
Zavodskaya Balka
(Arkadiev et al., 2010)
Berriasian
F. boissieri
Berriasian stratotype (France)
(Galbrun, 1985)
Subzone
Magnetochronological scale
(Ogg and Hinnov, 2012)
Magnetic chrons
m
Ma
Berriasian
Fauriella boissieri
Tirnovella occitanica
B. jacobi
Beds with Zeillerina baksanensis
Beds with Symphythiris arguinensis
Riasanites crassicostatum
Neocosmoceras euthymi
Dalmasiceras tauricum
Beds with Malbosiceras chaperi
grandis
Conorboides hofkeri
Lenticulina andromede
Triplasia emslandensis acuta
Quadratina tunassica
Lenticulina muensteri
Textularia crimica–Belorussiella taurica
Evirticyclammina virguliana, Rectocyclammina recta, Bramkampella arabica
Costacythere drushchitzi–Reticythere marfenini
Costacythere khiamii–Hechticythere belbekensis
Phoberocysta neocomica
B. callisto
B. picteti
M. paramimounum
D. dalmas
B. privasensis
T. subalpina
P. grandis
Tithonian
Subthurmannia boissieri
Subthurmannia occitanica
Berriasella jacobi
M14
M15
M16
M17
M18
M19
140
141
142
143
144
145

**Fig. 11.** Correlation of magnetostratigraphic data available for the Berriasian section of central and eastern Crimea with the Berriasian stratotype in southeastern France and standard magnetostratigraphic scale.

In the paleomagnetic column of the composite section of central Crimea, gaps 5 m wide and less in determinations of polarity are not shown. For legend, see Fig. 4.

This work was supported by the Russian Foundation for Basic Research (project nos. 11-05-00405-a, 13-05-00745-a, 14-05-31152_a_mol) and Ministry of Education and Science of the Russian Federation in the base part (project 1582) and the scientific field (project 1757).

*Reviewers M.A. Rogov, A.Yu. Kazanskii, and V.A. Zakharov*

## REFERENCES

Andreev, Yu.N. and Ertli, Kh.Yu., Some Cretaceous ostracods of Central Asia and related species of Europe, *Vopr. Mikropaleontol.*, 1970, no. 13, pp. 95–121.

Andreev, Yu.N., Cretaceous ostracods of Central Asia (composition, distribution, evolution, geological significance), *Doctoral (Geol.-Mineral.) Dissertation*, Moscow: MGU, 1986.

Arkadiev, V.V., Bagaeva, M.I., Guzhikov, A.Yu., et al., Bio- and magnetostratigraphic characterization of the Upper Berriasian section “Zavodskaya balka” (Eastern Crimea, Feodosiya), *Vestn. Sankt-Peterburg. Univ., Ser. 7. Geol. Geogr.,* 2010, Iss. 2, pp. 3–16.

Arkadiev, V.V., Stage subdivision of Berriasian deposits of Crimean Mountains, *Vestn. Sankt-Peterburg. Univ., Ser. 7. Geol. Geogr.*, 2007, Iss. 2, pp. 27–43.

Arkad’ev, V.V., Bogdanova, T.N., Lobacheva, S.V., et al., The Berriasian of Crimean Mountains: problems of zonal subdivision and correlation, in *Mat. Tret’ego Vseross. soveshch. “Melovaya sistema Rossii i blizhnego zarubezh’ya: problemy stratigrafii i paleogeografii”, Saratov, 26–30 sentyabrya 2006* (Proc. 3rd All-Russ. Conf. “The Cretaceous System of Russia and Adjacent Countries: Problems of Stratigraphy and Paleogeography”, Saratov, September 26–30, 2006), Musatov, V.A., Ed., Saratov: Izd-vo SO EAGO, 2006, pp. 18–20.

Arkadiev, V.V., Bogdanova, T.N., Lobacheva, S.V., et al., Berriasian Stage of the Crimean Mountains: Zonal subdivisions and correlation, *Stratigr. Geol. Correl.*, 2008, vol. 16, no. 4, pp. 400–422.

Arkadiev, V.V., Bogdanova, T.N., Guzhikov, A.Yu., et al., *Berrias Gornogo Kryma* (The Berriasian of the Crimean Mountains), St. Petersburg: Izd-vo “LEMA”, 2012 [in Russian].

*Atlas des Ostracodes de France*, Oertli, H.J., Ed., *Bull. Centre Rech. Explor.-Prod. Elf.-Aquit. Mem.*, 1985, no. 9.

Bagaeva, M.I., Arkadiev, V.V., Baraboshkin, E.Yu., et al., New data on bio- and magnetostratigraphy of Berriasian—Valanginian boundary deposit of Eastern Crimea, in *Paleontologiya, stratigrafiya i paleogeografiya mezozoya i kainozoya boreal’nykh raionov. Materialy nauchn. sessii (18–22 aprelya 2011 g.). T. I. Mezozoi* (Proc. Sci. Sess. “Paleontology, Stratigraphy, and Paleogeography of the Mesozoic and Cenozoic of the Boreal Regions” (April 18–22, 2011). Vol. I: Mesozoic), Novosibirsk: INGG SO RAN, 2011, pp. 23–26.

Baraboshkin, E.Yu., *Prakticheskaya sedimentologiya. Terrigennye rezervuary. Posobie po rabote s kernom* (Practical Sedimentology. Clastic Reservoirs. The manual on the core analysis), Tver: GERS, 2011 [in Russian].

Bogdanova, T.N., Lobacheva, S.V., Prozorovskii, V.A., and Favorskaya, T.A., On the Berriasian Stage subdivisions in the Crimean Mountains, *Vestn. Leningrad. Univ., Ser. Geol., Geogr.*, 1981, no. 6, pp. 5–14.

Bogdanova, T.N. and Kvantaliani, I.V., New Berriasian ammonites of the Crimea, *Byull. Mosk. O—va Ispyt. Prir., Otd. Geol.*, 1983, vol. 58, no. 3, pp. 70–83.

Buskirk, R. E. and O’Brien Jr., W. P., Magnetic remanence and response to magnetic fields in crustacea, in *Magnetite Biomineralization and Magnetoreception in Organisms*, Kirschvink, J.L., Jones, D.S., MacFadden B.M., Eds., New York, London: Plenum Press., 1985, pp. 365–383.

Debiche, M.G. and Watson, G.S., Confidence limits and bias correction for estimating angles between directions with applications to paleomagnetism, *J. Geophys. Res.*, 1995, vol. 100, no. B12, pp. 24405–24430.

Donze, P., Ostracodes berriasiens des subalpins septentrionaux (Bauges et Chartreuse), *Trav. Lab. Géol. Fac. Sc. Lyon. NS*, 1964, no. 11, pp. 103–158.

Donze, P., Especes nouvelles d’Ostracodes des couches de base du Valanginien de Berrias, *Trav. Lab. Géol. Fac. Sc. Lyon. NS*, 1965, no. 12, pp. 87–107.

*Dopolneniya k stratigraficheskomu kodeksu Rossii* (Supplements to the Stratigraphic Code of Russia), St. Petersburg: VSEGEI, 2000 [in Russian].

Drushchits, V.V. and Yanin, B.T., Lower Cretaceous deposits of the Central Crimea, *Vestn. MGU, Ser. Biol., Pochvoved., Geol., Geogr.*, 1959, no. 1, pp. 115–120.

Drushchits, V.V. and Gorbachik, T.N., Zonal subdivision of the Lower Cretaceous of the South of the USSR based on ammonites and foraminifers, *Izv. Akad. Nauk SSSR, Ser. Geol.*, 1979, no. 12, pp. 95–105.

Espitalie, J. and Sigal, J., Contribution a l’etude des Foraminiferas du Jurassique superieur et du Neocomien du Bassin de Majunga (Madagascar), *Ann. Geol. de Madagascar,* 1963, no. 32.

Feodorova, A.A., Reference sections of Jurassic—Cretaceous boundary sediments in the Crimea as a basis for detailed stratification and correlation of productive sequences in the Caspian shelf, in *Stratigrafiya neftegazonosnykh basseinov Rossii* (Stratigraphy of the Oil-and-Gas Basins in Russia), Vinogradov, N.V., Ed., St. Petersburg: Nedra, 2004, pp. 61–80.

Fisher, M.J. and Riley, L.A., The stratigraphic distribution of dinoflagellate cysts at the boreal Jurassic—Cretaceous boundary, *Proc. Fourth Int. Palynol. Conf., Lucknow*, 1980, no. 2, pp. 313–329.

Flügel, E., *Microfacies of Carbonate Rocks: Analysis, Interpretation, and Application. Second Edition*, Berlin, Heidelberg: Springer, 2010.

Galbrun, B., Magnetostratigraphy of the Berriasian stratotype section (Berrias, France), *Earth Planet. Sci. Lett.*, 1985, vol. 74, pp. 130–136.

Gorbachik, T.N. and Mokhamad, G.K., *Lituolida* Foraminifera from the Tithonian and Berriasian of the Crimea; structure, importance for stratigraphy and paleobiogeography, in *Problemy stratigrafii i paleontologii mezozoya* (Problems of Stratigraphy and Paleontology of the Mesozoic), Kozlov, G.E. and Prozorovskii, V.A., Eds., St. Petersburg: VNIGRI, 1999, pp. 165–186.

Gradstein, F., Ogg, J.G., Schmitz, M.D., and Ogg, G.M., *The Geologic Time Scale 2012*, Amsterdam: Elsevier, 2012.

Grekoff, N. and Magne, J., Les ostracodes du stratotype du Berriasien, *Rev. de Micropaleontol.*, 1966, vol. 9, no. 3, pp. 177–185.

Gründel, J., Neue ostracoden aus der deutschen Unterkreide II, *Monatsb. Deutschen Akad. Wiss. Berlin,* 1964, vol. 6, no. 11, pp. 849–858.

Guzhikov, A.Yu., Arkad'ev, V.V., Baraboshkin, E.Yu., et al., New sedimentological, bio-, and magnetostratigraphic data on the Jurassic-Cretaceous boundary interval of Eastern Crimea (Feodosiya), *Stratigr. Geol. Correl.*, 2012, vol. 20, no. 3, pp. 261–294.

Kolpenskaya, N.N., Ostracods. The Berriasian of Northern Caucasus (Urukh section), in *Biokhronologiya i korrelyatsiya fanerozoya neftegazonosnykh basseinov Rossii. Vyp. 2* (Biochronology and Correlation of the Phanerozoic of the Oil-and-Gas Basins of Russia), Kirichkov, A.I., Ed., St. Petersburg: VNIGRI, 2000, pp. 42–52, 115–129.

Kubiatowicz, W., Upper Jurassic and Neocomian ostracodes from Central Poland, *Acta Geol. Pol.*, 1983, vol. 33, nos. 1–4, pp. 1–72.

Kuznetsova, K.I. and Gorbachik, T.N., *Stratigrafiya i foraminifery verkhnei yury i nizhnego mela Kryma* (Upper Jurassic and Lower Cretaceous Stratigraphy and Foraminifers of the Crimea), Moscow: Nauka, 1985 [in Russian].

Kvantaliani, I.V. and Lysenko, N.I., On the problem of zonal subdivision of the Berriasian of the Crimea, *Soobshch. Akad. Nauk Gruz. SSR*, 1979, vol. 94, no. 3, pp. 629–632.

Lanza, R. and Meloni, A., *The Earth's Magnetism: An Introduction for Geologist*, Berlin-Heidelberg-New York: Springer, 2006.

Le Hégarat, G., Le Berriasien du Sud-East de la France, *Doc. Lab. Geol. Fac. Sci.*, 1973, vol. 43/1.

McFadden, P.L. and McElhinny, M.W., Classification of the reversal test in palaeomagnetism, *Geophys. J. Int.*, 1990, vol. 103, pp. 725–729.

Molostovskii, E.A., Eremin, V.N., Guzhikov, A.Yu., et al., Paleomagnetic stratigraphy of Mesozoic and Cenozoic deposits in southern and southeastern parts of the European USSR, in *Otchet o NIR po teme "Provesti detalizatsiyu i utochnenie magnitostratigraficheskoi shkaly mezozoya i kainozoya SSSR"* (Report on R&D Work: Detalization and Clarification of Magnetostratigraphic Scale of Mesozoic and Cenozoic of the USSR), Saratov: NII Geol. Saratov State Univ., 1989 [in Russian].

Monteil, E., Kystes de dinoflagelles index (Tithonique–Valanginien) du Sud-Est de la France. Proposition d'une nouvelle zonation palynologique, *Revue de Paleobiol.*, 1992, vol. 11, no. 1, pp. 299–306.

Morkhoven, F.P.C.M., Generic descriptions, in *Post-Paleozoic Ostracoda. Vol. II*, Amsterdam–London–New York: Elsevier, 1963.

Neale, J.W., Ostracoda from the Speeton Clay (Lower Cretaceous) of Yorkshire, *Micropaleontol.,* 1962, vol. 8, no. 4, pp. 425–484.

Neale, J.W., Ostracodes from the type Berriasian (Cretaceous) of Berrias (Ardeche, France) and their significance, *Univ. Kansas. Depart. Geol. Spec. Publ.*, 1967, no. 2, pp. 539–569.

Neale, J.W., The Cretaceous, in *A Stratigraphical Index of British Ostracoda*, Bate, R.N. and Robinson, E., Eds., *Geol. J. Spec. Iss.*, 1978, no. 8, pp. 325–384.

Nikishin, A.M., Bolotov, S.N., Baraboshkin, E.Yu., et al., Geological history of the Scythian-Black Sea Region, in *Ocherki geologii Kryma. Vyp. 1* (Essays on Geology of the Crimean Peninsula), Moscow: MGU, 1997, pp. 207–227.

Neale, J.W., Ostracodes from the Lower Valanginian of the Central Crimea, *Paleontol. Zh.*, 1966, no. 1, pp. 87–100.

Pecherskii, D.M. and Safonov, V.A., Palinspastic reconstructions of the position of Crimean Mountains in Middle Jurassic–Early Cretaceous based on the paleomagnetic data, *Geotektonika*, 1993, no. 1, pp. 96–105.

Pokorny, V., The ostracoda of the Klentnice Formation (Tithonian?), Czechoslovakia, *Rozp. Ustred. Ust. Geol.*, 1973, vol. 40, pp. 1–107.

*Prakticheskoe rukovodstvo po mikrofaune. T. 7. Ostrakody mezozoya* (Practical Manual on Microfauna. Vol. 7. Mesozoic Ostracoda), Nikolaev, I.A. and Neustruev, I.Yu., Eds., St. Petersburg: VSEGEI, 1999 [in Russian].

Raevskaya, E.G. and Shurekova, O.V., Modern technology and equipment for palynological analysis of carbonate-terrigenous deposits, in *Problemy sovremennoi palinologii. Materialy XIII Rossiiskoi palinologicheskoi konferentsii* (Proc. XIII Russ. Palynol. Conf. "Problems of Modern Palynology"), Syktyvkar: Inst. Geol. Komi NTs UrO RAN, 2011, pp. 103–107.

Slipper, I.J., Marine Lower Cretaceous, in *Ostracods in British Stratigraphy*, Whittaker, J.E. and Hart, M.B., Eds., *Publ. Micropaleont. Soc. Geol. Soc. London,* 2009, pp. 309–344.

Stolz, J.F., Chang, S.B.R., and Kirschvink, J.L., Bacterial magnetite as trace fossil and paleooxygen indicator, *Origins of Life and Evolution of the Biosphere*, 1986, vol. 16, nos. 3–4.

Tavera, J.M., Los ammonites del Tithonico Superior-Berriasense de la zona Subbetica (Cordilleras Beticas). Tesis Doctoral, Granada: Univ. Granada, 1985.

Tesakova, E.M. and Rachenskaya, L.P., New Ostracodes (Crustacea, Ostracoda) of the Genus Costacythere Gründel from Berriasian sediments of the Crimea, *Paleontol. Zh.*, 1996, vol. 30, no. 4, pp. 416–428.

Tesakova, E.M. and Rachenskaya, L.P., New Ostracodes (Crustacea, Ostracoda) of the genera *Bairdia* M'Coy, *Neocythere* Mertens, *Macrodentina* Martin, *Hechticythere* Gründel, and *Cypridea* Bosquet from the Berriasian of Central Crimea, *Paleontol. J.*, 1996, vol. 30, no. 5, pp. 542—551.

Triebel, E., Ostracoden untersuchungen, *Protocythere* und *Exophtalmocythere*, zwei neue Ostracoden gattungen aus der Deutschen Kreide, *Senckenbergiana Lethaea*, 1938, vol. 20, no. 1/2, pp. 179–199.

Tucker, M.E. and Wright, V.P., *Carbonate Sedimentology*, Oxford: Blackwell Science, 1990.

Van der Voo, R., *Palaeomagnetism of the Atlantic, Tethys, and Iapetus oceans*, Cambridge: Cambridge Univ. Press, 1993.

Williams, G.L., Dinoflagellate and spore stratigraphy of the Mesozoic–Cenozoic, Offshore Eastern Canada, *Geol. Surv. Canada*, 1975, Pap. 74–30, pp. 107–161.

Wright, V.P. and Burgess, P.M., The carbonate factory continuum, facies mosaics and microfacies: an appraisal of some of the key concepts underpinning carbonate sedimentology, *Facies*, 2005, vol. 51, pp. 17–23.

Yampolskaya, O.B., Paleomagnetism and petromagnetism of Lower Cretaceous deposits of Crimean Mountains: stratigraphic and paleogeographic aspects, *Cand. Sci. (Geol.-Mineral.) Dissertation* , Saratov: SGU, 2005.

Yampolskaya, O.B., Baraboshkin, E.Yu., Guzhikov, A.Yu., et al., Lower Cretaceous paleomagnetic section in the southwest Crimea, *Moscow Univ. Geol. Bull.*, 2006, vol. 61, no. 1, pp. 1–16.

Yanin, B.T. and Smirnova, T.N., Stratigraphic distribution of bivalves and brachiopods in Berriasian and Valanginian deposits of the Crimea, *Byull. Mosk. O-va Ispyt. Prir., Otd. Geol.*, 1981, vol. 56, no. 1, pp. 82–94.

Yanin, B.T. and Baraboshkin, E.Yu., The Berriasian section in the Bel'bek River Basin, Southwestern Crimea, *Stratigr. Geol. Correl.*, 2000, vol. 8, no. 2, pp. 165–176.

*Translated by I. Basov*